Chemical and Biological Hazard Prevention

Studies and Research Projects

REPORT **R-849**

The Effect of Upstream and Downstream Buildings on Dispersion of Effluents

A Computational Fluid Dynamics (CFD) Approach

Ali Bahloul
Ted Stathopoulos
Mauricio Chavez
Bodhisatta Hajra

irsst

The Institut de recherche Robert-Sauvé en santé et en sécurité du travail (IRSST), established in Québec since 1980, is a scientific research organization well-known for the quality of its work and the expertise of its personnel.

OUR RESEARCH is *working* for you !

Mission

To contribute, through research, to the prevention of industrial accidents and occupational diseases and to the rehabilitation of affected workers;

To disseminate knowledge and serve as a scientific reference centre and expert;

To provide the laboratory services and expertise required to support the public occupational health and safety network.

Funded by the Commission de la santé et de la sécurité du travail, the IRSST has a board of directors made up of an equal number of employer and worker representatives.

To find out more

Visit our Web site for complete up-to-date information about the IRSST. All our publications can be downloaded at no charge.
www.irsst.qc.ca

To obtain the latest information on the research carried out or funded by the IRSST, subscribe to *Prévention au travail,* the free magazine published jointly by the IRSST and the CSST.
Subscription: *www.csst.qc.ca/AbonnementPAT*

Legal Deposit
Bibliothèque et Archives nationales du Québec
2014
ISBN: 978-2-89631-768-4 (PDF)
ISSN: 0820-8395

IRSST – Communications and Knowledge Transfer Division
505 De Maisonneuve Blvd. West
Montréal, Québec
H3A 3C2
Phone: 514 288-1551
Fax: 514 288-7636
publications@irsst.qc.ca
www.irsst.qc.ca

Chemical and Biological Hazard Prevention

Studies and Research Projects

REPORT **R-849**

The Effect of Upstream and Downstream Buildings on Dispersion of Effluents

A Computational Fluid Dynamics (CFD) Approach

Ali Bahloul,
Chemical and Biological Hazards Prevention,
IRSST

Ted Stathopoulos, Bodhisatta Hajra, Mauricio Chavez
Department of Building, Civil and Environmental Engineering,
Concordia University

Clic Research
www.irsst.qc.ca

A PDF version of this publication is available on the IRSST Web site.

This study was funded by the IRSST. The conclusions and recommendations are solely those of the authors.

PEER REVIEW

In compliance with IRSST policy, the research results published in this document have been peer-reviewed.

ACKNOWLEDGEMENTS

This work was supported by the Institut de recherche Robert-Sauvé en santé et en sécurité du travail (IRSST) du Québec. The cooperation, support and encouragement of IRSST, which were instrumental in the success of the research, are acknowledged with sincere thanks.

ABSTRACT

The prediction of pollutant dispersion from rooftop emissions in an urban environment is an extremely complex phenomenon particularly in the vicinity of a group of buildings. The plume behaviour depends on the wind characteristics but is also severely affected by the surroundings. This causes effluents released from stacks located on one of the buildings to re-enter the same or an adjacent building, causing potential health problems to its occupants. The optimal design and placement of exhaust stacks to limit this re-ingestion on air intakes and other sensitive locations can be a considerable challenge. Unfortunately, the state-of-the-art of dispersion modeling, particularly around a non-isolated building configuration, is not sufficiently advanced for accurate predictions in order to avoid such situations. Therefore, there is a need to develop a new model or modify an existing model to take into account the effects of dispersion of effluents and in particular focus on the impact of buildings that are in close proximity of the source of pollutants. To address this issue, a collaborative research program between Concordia University and IRSST was elaborated relying both on experimental and numerical modeling. The experimental findings have been published in a companion report[1] (Stathopoulos *et al.* 2014) while the current report focuses on the numerical modeling phase of the research.

The purpose of this study was to contribute to a better understanding of air pollution aerodynamics in urban areas by focusing on the most representative non-isolated building configurations: a building located upstream of an emitting building, a building located downstream of an emitting building and two buildings, one located upstream and the other one located downstream of an emitting building. All these cases were compared with a reference case: an isolated emitting building. The effect of adjacent buildings on the near field of a pollutant source was analysed in terms of dilution distribution on the roof of an emitting building.

The current research methodology uses Computational Fluid Dynamics (CFD) to study pollutant dispersion in the vicinity of a cluster of buildings. This tool provides detailed information on flow pattern and concentration (or dilution) fields by solving the flow equations in the entire computational domain. Numerical simulation reliability is one of the main concerns of this study; therefore, validation of results through comparisons with wind tunnel data collected during the experimental phase conducted at Concordia University is included in this report. Mesh quality, boundary conditions, turbulence model choice, wall treatment and numerical parameters are some of the elements that can be calibrated through comparison with experimental data.

To achieve our objective, two steps are suggested; the first step is to generate sufficient information regarding the setup of CFD simulations for flow and dispersion in urban areas. Special attention is paid to transport processes in order to build the best numerical model possible for such applications. The second step is a parametric analysis for diverse cases of pollutant dispersion in an urban area. The results are presented in terms of normalized dilution at roof level of an emitting building, but also as iso-contour planes of dilution field and stream lines showing the airflow pattern of all the configurations analysed. From the first step it was observed that in general steady CFD simulations tend to underestimate dilution when comparing with

[1] http://www.irsst.qc.ca/media/documents/PubIRSST/R-848.pdf

wind tunnel results. This underestimation is probably caused by the inherent incapability of RANS to capture unsteadiness of the flow. An adjustment in the value of turbulent Schmidt number (Sct) permits to obtain a better agreement with experiment data. In fact, reducing Sct permits to increase turbulent diffusion and then increase dilution of the pollutant. The parametric analysis (second step) produced valuable information about scalars and velocity fields as well as about vortical structures formed in the leeward side and between buildings. Knowing how these flow characteristics interact with the surroundings is essential to improve the understanding of pollutant dispersion within an urban area.

TABLE OF CONTENTS

LIST OF TABLES

LIST OF FIGURES

NOMENCLATURE

Symbol	Definition	Units
Ce	Exhaust concentration	ppm
Cr	Receptor concentration	ppm
Dr	Dilution at roof level (Ce/Cr)	
D_N	Normalised dilution	
D_t	Turbulent mass diffusivity	m^2/s
H	Building height	m
$TI_{u/v/w}(y)$	Turbulence intensity in x, y, z, direction at given y (m)	
k	Turbulent kinetic energy	m^2/s^2
k_s	Roughness height	m
K	Non-dimensional concentration	
M	Exhaust momentum ratio (V_e/ U_H)	
Q_e	Volumetric flow rate	m^3/s
Re	Reynolds number	
Sct	Turbulent Schmidt number	
t	time	s
U,V,W	velocity vector in x, y, z, direction	m/s
x	streamwise coordinate	m
y	vertical coordinate	m
Y^+	Dimensionless wall distance	
z	lateral coordinate	m
z_o	Aerodynamic roughness length	m

LIST OF SYMBOLS AND ABBREVIATIONS

Greek symbols	Definition	Units
α	Power law exponent	
ε	Turbulent dissipation rate	m^2/s^3
κ	von Karman constant	
ν_t	Turbulent viscosity	m^2/s
ρ_e	Density of exhaust	kg/m^3
ρ_a	Density of air	kg/m^3

Abbreviations

ABL	Atmospheric boundary layer
ADMS	Atmospheric Dispersion Modelling System
ASHRAE	American Society of Heating Refrigeration and Air conditioning Engineers
CFD	Computational Fluid Dynamics
GC	Gas Chromatograph
LES	Large Eddy Simulation
RANS	Reynolds-Averaged Navier-Stokes
RNG	Renormalized Group k-ε
RLZ	Realizable k-ε
RSM	Reynolds Stress-Model
SGS	Subgrid scale
STD	Standard k-ε
URANS	Unsteady Reynolds-Averaged Navier-Stokes

1. INTRODUCTION

1.1 Background

There is an increasing concern about the health hazards posed to urban occupants exposed to inhalation of fine and ultrafine particles, including microorganisms, dust and nano-technological products. Inhaling these particles causes an occupational hazard due to the elevated amount emitted to the atmosphere and working environment by vehicular traffic, industries, laboratories, hospitals and central cooling systems. The permanent growth of industrialized cities led government organizations and scientists to engage into preventive and remedial initiatives to eliminate or reduce negative effects on people's health of this called urban air pollution.

The transport of pollutants within the built environment is influenced by many complex factors. Among others, the most relevant factors affecting pollutant dispersion are the wind conditions and the urban morphology. The former refers to the wind speed and turbulence intensity. The higher the wind speed, the greater the mixture between fresh air and pollutants, and the lower the concentration of pollutants (or higher the dilution) that is detected in the wind stream. In its turn, complex urban morphology enhances vortical structures in the wake of buildings. Indeed, these recirculation zones tend to trap pollutants increasing local concentration, which may be very critical if the building fresh air intakes are located in these contaminated zones increasing the possibility of having ingestion of pollutants (Snyder, 1981, Schulman *et al.* 1993, Saathoff *et al.* 2009, Stathopoulos *et al.* 2004, 2008). This episodic phenomenon is present in all highly dense urban areas; however limited information and recommendations are available in the literature to avoid such problems. To limit air indoor contamination caused by the ingestion of outdoor pollutants, a better understanding of pollutant aerodynamics and transport mechanisms is needed.

The current report is the second of a collaborative research project carried out by the IRSST and Concordia University on dispersion of pollutant field. The first report of this research project (Stathopoulos *et al.* 2014) presented an extensive wind tunnel database of pollutant dispersion with different configurations for an isolated and a non-isolated emitting building. The findings of that other report were used to generate correction factors to improve the ASHRAE dispersion model. The main purpose of the present report is to study and validate a numerical approach for the dispersion of pollutant studies.

Computational Fluid Dynamics (CFD) is a useful technique for dispersion simulations since it provides detailed information of flow patterns and concentration fields by solving the flow equations at the entire computational domain. Even though CFD is largely used for research, it needs to be treated with care since it can be a source of significant errors conditioning the suitability of simulation results. The current report includes a comprehensive review of most relevant computational parameters in order to ensure reliability of the results. The present study puts in perspective the advantages and the disadvantages of using CFD for parametric studies on pollutant dispersion in urban areas. The following section describes in detail the objectives of the present work.

The current project belongs to Chemical and Biological Hazards Prevention which is one of the four research fields that IRSST has defined as priorities. More precisely, this project satisfies the necessity of developing strategies and methods to evaluate and control the worker exposure to chemical and biological agents spread in the air. The numerical methodology proposed in the current work is a valuable tool for complex studies on air quality and industrial ventilation problems.

1.2 Objectives

The main objective of this report is to establish a reliable method to study the effect of adjacent buildings on the dispersion of effluents using the Computational Fluid Dynamics (CFD) approach.

The specific objectives are as follows:

- To improve the accuracy and reliability of CFD to predict pollutant dispersion in urban areas. To this end, systematic comparisons with wind tunnel data were carried out. The comparisons allowed the identification of the necessary parameters and conditions that needed to be adjusted for the successful evaluation of CFD to resolve dispersion problems.
- To conduct a brief parametric study of dispersion for different building configurations focusing on the effect of adjacent buildings. The goal was to identify the dominant parameters affecting the dispersion of pollutants in the vicinity of an emitting building. Four cases were examined:
    i. Isolated emitting building (source);
    ii. Buildings of different geometries placed upstream of the source;
    iii. Buildings of different geometries placed downstream of the source;
    iv. One building placed upstream and another building placed downstream of the source.
- To produce relevant qualitative and quantitative information in the near field of an emitting building information to contribute to the better understanding of pollutant aerodynamics within the intra-urban scale.

Following the introduction in the current Chapter, a detailed literature review is presented in Chapter 2, describing previous studies carried out in the area of near-field plume dispersion using CFD. Chapter 3 describes the methodology and CFD setup, followed by results and discussion in Chapter 4. Finally the conclusions and recommendations for future work are presented in Chapter 5, followed by a list of references and appendices.

2. LITERATURE REVIEW

2.1 General

The accurate prediction of pollutant dispersion in urban areas does not just require the understanding of air pollution meteorology, but also needs a good understanding of urban aerodynamics. The extreme complexity of air flow in the city is conditioned by local geometry (building density, building heights distribution, street configuration, etc.) and local topology as well. For this reason, a good understanding of fluid mechanics applied on urban wind field is necessary for future improvements in models and methods (Cermak *et al.* 1995). Pollutant dispersion prediction has been addressed using mainly three methods: wind tunnel experiments, semi empirical formulations and Computational Fluid Dynamics simulations (CFD). In this section a brief description of wind tunnel and semi empirical formulation will be discussed followed by a detailed review of the CFD approach for pollutant dispersion studies.

2.2 Wind tunnel experiments

Wind tunnel modelling has been largely used to study the flow characteristics associated with bodies that are completely immersed in a moving flow. This approach allows simulation of flow in complex building geometries including the effects of surrounding structures and local topology. Meroney (2004) defines wind tunnel or water tunnel as analog computers which have the advantage of “near infinitesimal” resolution and “near–infinite memory”. Furthermore, this model approach employs “real fluids” with real properties and behaviour, where flow separation and recirculation are automatically taken into account without any kind of approximation. Although wind tunnel studies are useful in predicting plume dilutions, time and financial constraints are two of the major disadvantages associated with them (Blocken *et al.* 2008).

2.3 Semi empirical formulations: Gaussian based models

The Gaussian model is a mathematical (normal) distribution of pollutant concentration emitted from stacks in the vertical and crosswind directions. It is the basic workhorse for dispersion and it is the one most commonly used because: 1) it produces results that agree well with experimental data, 2) it is fairly easy to use and 3) it is consistent with the random nature of turbulence (Hanna, 1982). This model does not consider site-specific geometries that may substantially alter plume behaviour; thus this approach is not applicable for complex buildings or locations where other buildings are nearby, which is the case in urban areas.

Currently, the American Society of Heating, Refrigerating and Air Conditioning Engineers (ASHRAE, 2011) develops standards for designers dealing with the design and maintenance of indoor environments (http://www.ashrae.org). The *ASHRAE Applications Handbook*, Chapter 45, gives guidelines for determining plume dilutions for an isolated building, i.e. without considering the effects of adjacent buildings. The improvement of these standards and guidelines has been the purpose of the companion report (Stathopoulos *et al.* 2014).

2.4 CFD for pollutant dispersion

Computational Fluid Dynamics (CFD) is the analysis of fluid flow, heat, mass transfer and associated phenomena such as chemical reactions by solving a subset of traditional Navier Stokes equations at finite grid locations. It provides results of the flow features at every point in space simultaneously. Based on fundamental physics, CFD is used in a wide range of fundamental research and practical applications. In urban wind engineering, CFD has emerged as a promising technology due to the flexibility to model complex geometries such as cities with dense high-rise buildings. CFD is not intrinsically limited by similitude constraints (as wind tunnel) and therefore it should be possible to numerically simulate all aspects of pollutant dispersion and its interactions with the surroundings (Meroney, 2004). Even though, CFD offers some advantages compared with methods previously mentioned, it requires specific care in order to provide reliable results. A number of parameters such as grid size, discretization scheme, choice of turbulence model, boundary conditions must be verified and validated by systematic comparison with experimental data or other high accuracy methods (Blocken *et al.* 2008).

Since the seventies, computational wind engineering, as a branch of computational fluid dynamics, has been developed rapidly to simulate the airflow around buildings. However, applications of CFD to air pollution really began with prediction of wind flow and mass transport over an isolated cubic or other simple-shaped model. The isolated cubic building is a textbook case; it is used as a benchmarking process to compare different approaches and methods for dispersion prediction.

One of the first studies involving the complexity of flow field around a bluff body (representing an isolated building) and the relative performance of various turbulence models were conducted by Murakami and Mochida (1988). In this study, velocity distribution from three-dimensional steady state simulations of flow around a cubic model were compared with wind tunnel results to examine the accuracy of Standard k-ε turbulence model. The distribution of turbulent kinetic energy (k) was examined and it was found that the level of the production of k around the windward corner was significantly overestimated. The study suggested further efforts including the modification of turbulence modelling in the k-e model.

In a subsequent study, Murakami (1993) showed that flow fields around bluff bodies are characterized by complex distributions of the strain-rate tensor, which is highly anisotropic and changes significantly depending on the relative position of the bluff body. He revealed that the overestimation of turbulent kinetic energy, produced by the Standard k-ε model, is improved using the unsteady Large Eddy Simulation (LES). He concluded that one of the most distinct differences between Standard k-ε and LES is the modelling of the production term of turbulent energy. He concluded that LES has a great potential in flow prediction around buildings.

Brzoska *et al.* (1997) using a fourth-order accurate finite element code, compared wind tunnel measurement with Standard k-ε model simulation of releases from a stack located within the recirculation zone behind the building. The purpose of this work was to quantify the effect of stack velocity on the concentration in the recirculation. The study verified that pollutant mass in the recirculation zone decreases considerably at high stack velocity. The fraction captured will

depend on the wind speed and its profile, the building size and shape, as well as the discharge characteristics. The paper presented a strategy for estimating the fraction of pollutant captured by the recirculation for the case of a discharge within the wake. Finally, as previous researchers found, the authors confirmed that Standard k-ε model yields large values of turbulent kinetic energy at the front corner of the building, which results in reduction or elimination of the recirculation zone on the top of the building due to the excessive diffusion. In the recirculation zone behind the building, the turbulent kinetic energy is underestimated resulting in less diffusion with a subsequent increase in the recirculation cavity.

Meroney *et al.* (1999) studied flow field and dispersion about several building shapes. The study compared the turbulent models Standard k-ε, Renormalization Group (RNG) k-ε and Reynold's Stress Model (RSM) incorporated in Fluent (a commercial CFD code) with wind tunnel measurements. The intent of these comparisons was to determine if relatively robust commercial software could be used to simulate properly wind engineering problems. It was observed that numerical simulation consistently over-predicts surface concentrations downwind of the source locations. The study considered these discrepancies as a consequence of the impossibility of Reynolds-averaged numerical model to replicate the intermittency of flow in recirculation zones visualized in the wind tunnel. Then, even if the concentration patterns were well reproduced, magnitudes were frequently an order-of-magnitude larger than those of wind tunnel measurements. Concerning pressure patterns, it was shown that numerical predictions were reasonably accurate and magnitudes were close enough to permit engineering calculations. This suggests that mean pressure fields are less sensitive to numerical model details than other criteria. Finally, it was found that RSM turbulence models produced somewhat more realistic results than Standard k-ε or RNG models.

Flowe and Kumar (2000) performed a parametric study to determine the length of the recirculation cavity as a function of the ratio of building width to building height both in front of and in the rear of the building. The purpose of his study was to investigate the feasibility of using a three-dimensional k-ε numerical model as a means of modelling airflow past a building and stack geometry. The collected dispersive data were then used to determine new correlations between the ratio of building width to building height and the recirculation cavity size and average concentration in the rear recirculation cavity.

Castro (2003) pointed out the fact that an isolated building, which is the physical model used in the majority of dispersion studies around buildings, is a practical rarity because any site of interest generally contains a number of structures or, at least, has other buildings not far away from the one of interest and certainly within the expected range of influence. Additionally, surface pressures and local wind fields depend crucially on the characteristics of the upstream flow, so it is important to simulate the upstream boundary layer properly. This requires a careful match between the turbulent model parameters and the rough surface boundary conditions. The study also confirmed that Standard k-ε turbulence model is totally inadequate for flows around bluff bodies, because it always gives too much generation of turbulent kinetic energy just upstream of the impingement regions, resulting in inaccurate levels of surface pressures, particularly near the leading edges. The study proposed significant improvements by using appropriate ‘fix-ups’ to the k-ε or by using differential stress turbulence models, but it remains unclear to what extent the very strong suctions at leading edges and corners can be simulated. It

should be noted that the use of more sophisticated turbulence models, generally requires the use of significantly finer grids and more accurate numerical schemes.

The discrepancies observed in the k-ε Reynolds-Averaged Navier-Stokes (RANS) model were examined by Cheng *et al.* (2003) who compared Standard k-ε model with LES model of a fully developed turbulent flow over a matrix of cubes (resembling an array of buildings). The results of his investigation proved that both models give reasonably good qualitative results. For instance, flow structures including a horseshoe at the front face of the cube that wraps around the side wall, an arch-shaped vortex in the wake, and thin separation bubbles on the rooftop and side walls were observed. Quantitatively, the profiles of mean velocity were generally better represented by LES model. In fact, the k-ε RANS model produced a severe underestimation of the mean streamwise velocity component in the horseshoe vortex region just upstream of the lower part of the front face of the downstream cube. This, in turn, creates much thicker boundary layers on the side. The complex features of flow within and above the cubes array (e.g. vortex shedding, large separation zones, topology of reattachment lines bordering the recirculation regions, fine-scale flow structures near the side walls, etc.) are reproduced better with the LES model. Clearly, the advantages of LES model are quite evident compared with the k-ε RANS model; however the computational cost (run time) is also significantly higher. In this study, the computational cost associated with LES model is about 100 times greater than that incurred with the k-ε RANS model.

Liu and Ahmadi (2006) studied the particle transport, dispersion and deposition near a building using a Lagrangian particle tracking approach. The computational model accounted for the drag and lift forces acting on the particle, as well as the effect of Brownian force, in addition to the gravitational sedimentation effects. A point source of helium gas was chosen to serve as the contaminant source and the helium concentration in the plane behind the building and perpendicular to the direction of airflow was evaluated. The results showed that the deposition and dispersion of 0.01 and 1μm particle were similar. The gravitational force had a significant effect on the deposition rate of 10 μm particles. The comparison with the available data showed an agreement for the mean airflow and gas concentration.

Olvera *et al.* (2008) studied the recirculation cavity behind a cubical building using a commercial CFD code and the RNG k-ε turbulence model. It was observed that plume buoyancy affects the size and shape of the cavity region of flow structure and concentrations within it. The paper recommends including this effect in the downwash algorithm in order to improve the accuracy of modelling results for far-field concentration distributions. Indeed, this would be mandatory in accident assessments, where accurate predictions of short-term, near-field concentration fluctuations near source releases are required.

The inaccuracies of dispersion prediction associated to Standard k-ε models and the effects of turbulent Schmidt number (Sct) were analysed by Tominaga and Stathopoulos (2007). Sct is necessary to solve the transport mass equation in CFD prediction of dispersion with k-ε RANS model; it is defined as the ratio of turbulent momentum diffusivity (eddy viscosity) to the mass diffusivity ($Sct = \nu t/Dt$). The paper emphasized on the issue that Sct has a significant effect on dispersion predictions since it appears in the turbulent diffusion hypothesis, which is used to estimate the turbulent mass flow. A smaller value of Sct tends to provide better predicted results

on concentration distributions around an isolated building using Standard k-ε model. It was concluded that the systematic underestimation of turbulent diffusion of momentum by k-ε RANS model can be compensated using an appropriate smaller Sct. However, to pronounce a clear statement for the optimum Sct remains not possible due to the strong flow characteristic dependence of Sct.

Di Sabatino *et al.* (2007) verified the effect of Sct for flow within a small building arrangement and pollutant dispersion in street canyons. The study compared Standard k-ε model with the atmospheric dispersion model ADMS-Urban. Similarly, with previous researchers, it was found that the concentration in the street canyons is overestimated. The authors explained this overestimation as a consequence of the lower turbulent kinetic energy (k) levels obtained in CFD simulations near the buildings. Finally, it was also mentioned that dispersion can be artificially increased by lowering the Sct.

Tominaga and Stathopoulos (2009) tested different turbulent models for flow and dispersion around an isolated cubic building. Standard k-ε was again found to be inadequate for concentration prediction because it cannot reproduce the basics of flow structure, for instance reverse flow on the roof. However, the RNG k-ε and Realizable models provided much better agreement with experimental data using Sct = 0.3. It was confirmed that the underestimation of turbulent diffusion for momentum can be compensated by small value of Sct.

The various research studies presented in this section show that studies concerning pollutant dispersion in urban areas have been focused on the isolated building case. Some publications have found that, in general, CFD simulations show good agreement with experimental measurements in terms of flow pattern. However, using the steady state RANS model an underestimation of dispersion in the proximity of the source is always observed for the isolated building case. Some authors explained this underestimation as a consequence of the impossibility of RANS to replicate the intermittent nature of bluff body flow. It is also explained that the underestimation of dispersion by RANS is a consequence of low turbulent momentum diffusion predicted near the building. To compensate for this underestimation, a calibration is possible by decreasing the value of Sct. However, it is clear that changes on Sct value cannot be generalized considering the particular flow characteristics of each case. Presently, a discussion about whether a Sct calibration is valid to improve pollutant dispersion is currently open as it can be found in various publications (Di Sabatino *et al.* 2007; Tominaga and Stathopoulos, 2007; Blocken *et al.* 2008; Chavez *et al.* 2011).

3. METHODOLOGY

3.1 General

The current study is based mainly on CFD simulations; however wind tunnel experiments were used for validation purposes. The methodology concerning CFD use is described in the present section as well as some general aspects of wind tunnel experimentation.

3.2 CFD simulations

The aim of the numerical prediction is to solve the governing set of partial differential equations that describe any kind of fluid flow, such as wind flow in the atmosphere. These equations are based on the fundamental laws of conservation of mass and momentum (Navier-Stokes equations) within the calculus domain (Fluent User Guide, 2001).

3.2.1 Physical model representation and computational domain

Since the present numerical simulation results are validated using wind tunnel data, it is crucial to numerically reproduce the wind tunnel as much as possible. In consequence, all the numerical models included in the present report have the same reduced scale that the wind tunnel physical models have. The numerical building models are represented by simple shapes as cuboid and the computational domain as a parallelepiped. Based on recommendations from past studies, the dimensions of this numerical domain were specified as follows: considering H as the height of the taller building in the model, the lateral and the top boundary were 5H away from the building and the outlet boundary was 20H downwind from the building to allow flow development (Tominaga and Stathopoulos, 2009). For the inlet, a distance of 3H was adopted in order to minimize the development of streamwise gradients, as discussed in Blocken *et al.* (2008).

3.2.2 Meshing

The meshing was constructed principally using structured hexahedra grids since it has been proven that this mesh style provides the best computational results (Hefny and Ooka, 2009). The expansion ratio between two consecutive cells was limited to 1.25 as suggested by Franke *et al.* 2007. A mesh sensitivity study was conducted in order to define the optimum mesh characteristics and size.

The meshing study was based on a basic literature case represented by a cubical building with an exhaust vent at the roof. The reason to use this single cube, instead of the actual emitting building used all along this report, was because the cube model is a well-known case for which experimental data from Li and Meroney (1983) were available. Numerical studies based in the same cube are available in the literature as the dispersion study conducted by Blocken *et al.* (2008). In this section, the single cube case was reproduced and analyzed to establish an acceptable meshing procedure for subsequent numerical simulations.

The building model is a 0.05 m cube in a wind tunnel with M=0.07. Please note that M is the exhaust momentum ratio, defined as the ratio between the exhaust velocity and the mean wind speed at the building height: $M=V_e/U_H$ (where V_e is the exhaust velocity). The numerical model was conducted using the same physical dimensions and computational boundary conditions used by Blocken *et al.* (2008). The grid was generated using hexahedral elements and five meshes were created, as shown in Figure 3.1 and detailed in Table 1. High concentrations of cells were placed in the vicinity of the building vent.

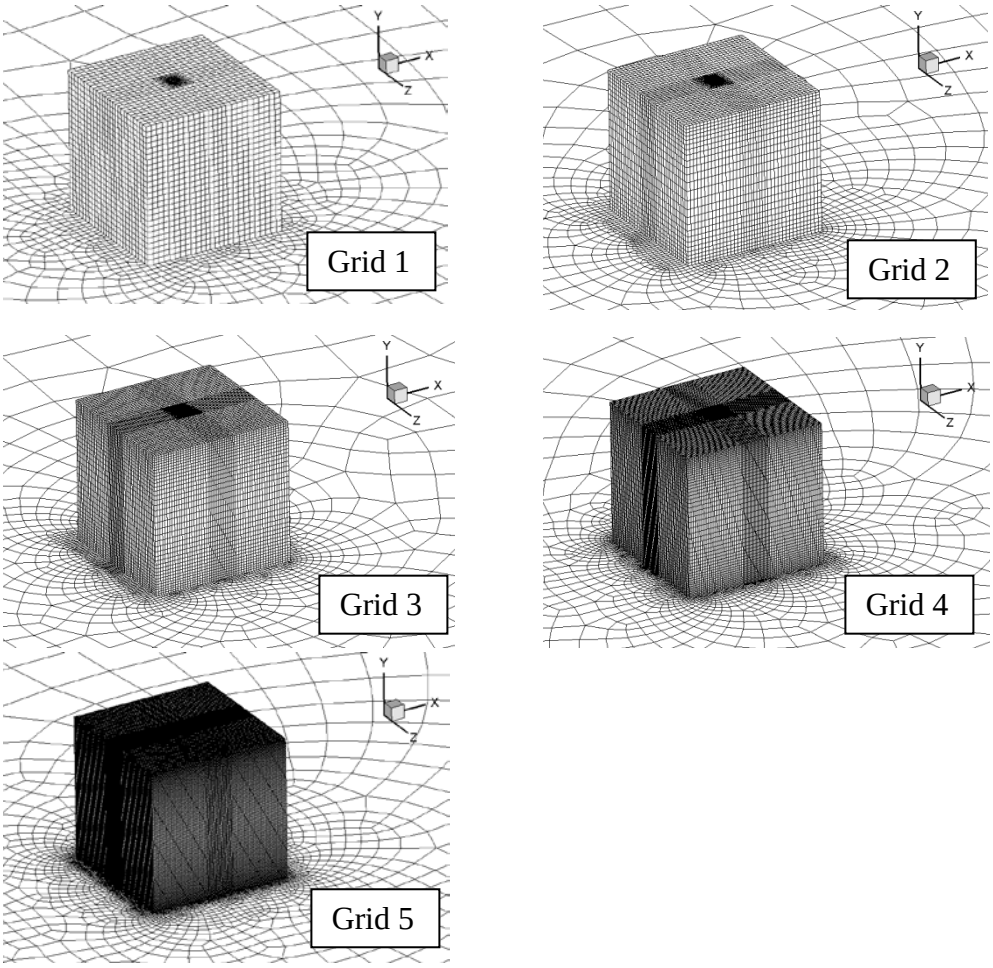

Figure 3.1 – Different sizes of meshing for a cube.

Table 1 : Details of meshing.

	Size	Y^+ (bldg. roof)	Y^+ (bldg. wall)	Y^+ (ground)
Grid 1	112,528	9.9	9.6	10.1
Grid 2	206,143	6.2	6.9	6.4
Grid 3	**442,370**	**4.7**	**5.0**	**4.4**
Grid 4	959,394	3.1	3.7	2.6
Grid 5	2,467,595	2.1	2.8	1.5

The Realizable turbulence model was selected to compare meshing effects. It is important to note that the viscous sub-layer region ($Y^+ < 5$) was included in the simulation of the near-wall domain and solved using the Enhanced Wall Treatment (EWT) option available in Fluent (Fluent User Guide, 2001). Three vertical lines were defined to plot the velocity profile variation on three different locations: upwind, above and downwind the building, as shown in Figure 3.2. One horizontal line, identified as Line-h1, was used to plot a dimensionless concentration of a tracer gas at roof level of the building.

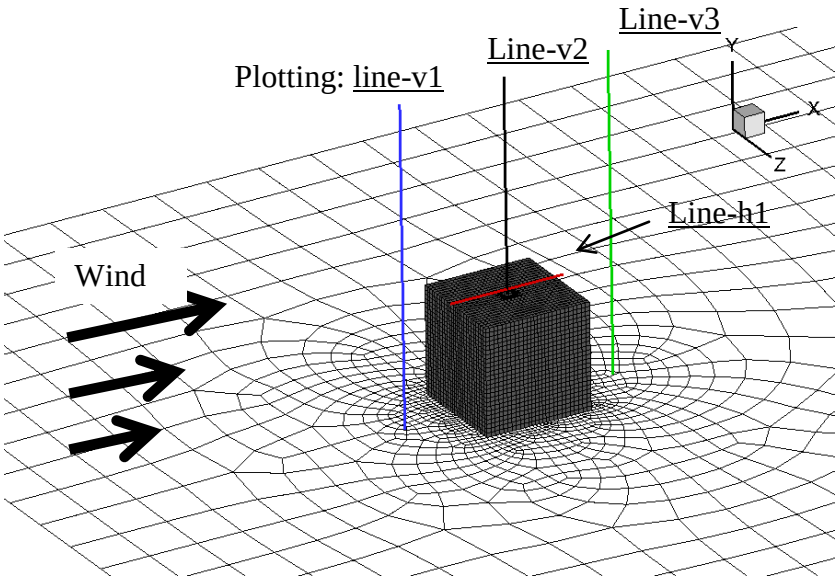

Figure 3.2 – Location of plotting lines.

Velocity profiles in the x-direction for the designated meshes and locations are plotted in Figure 3.3. It is noted that practically no difference in velocity values was detected for all the meshes on the three vertical lines. For the region downwind of the building (Figure 3.3b), known as the wake of the building, the negative values indicate the existence of a recirculation zone. Since the velocity values are almost identical, it is possible to assume that the size of this recirculation zone is identically computed for the five meshes. Consequently, the mesh, when using high

concentration of cells near the walls has no significant influence on the velocity field obtained numerically.

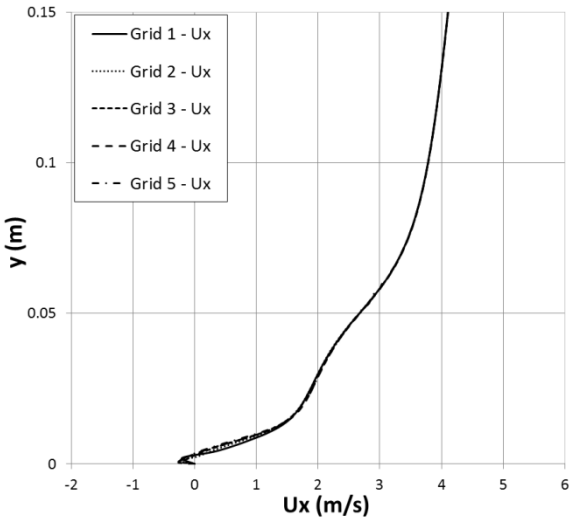

a) **Line 1**

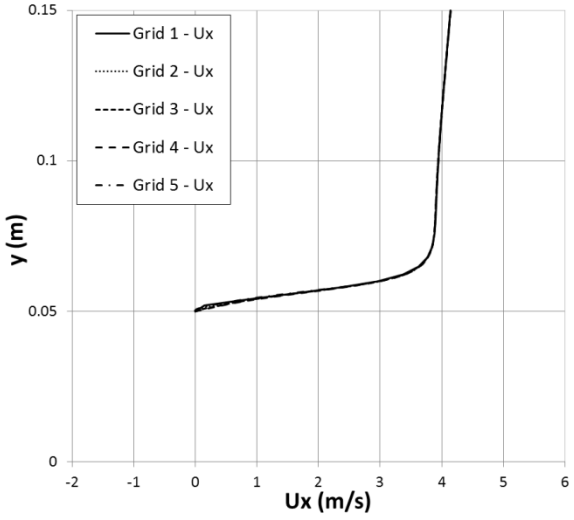

b) **Line 2**

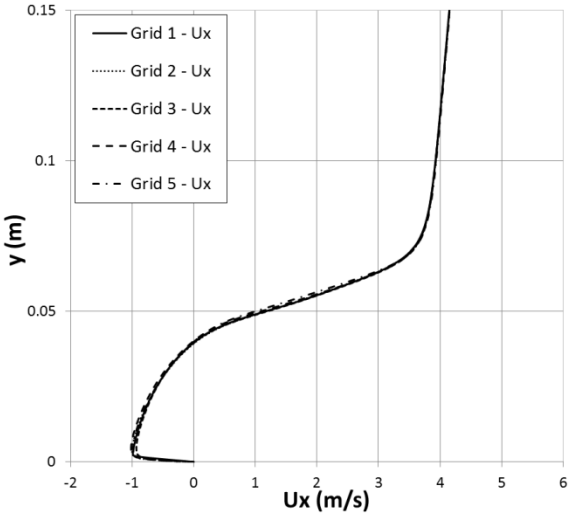

c) Line 3

Figure 3.3 – Velocity profiles along three vertical lines for different mesh sizes.

To evaluate the dispersion of pollutant, the normalized concentration K, defined below, was plotted along the horizontal line called Line-h1.

$$K = \frac{cH_b^2 U_b}{Q_c}$$

where H_b is the height of the building, U_b the wind speed at the building height, c the concentration obtained by CFD simulation and Q_c the flow rate from the vent.

Figure 3.4 compares K obtained in the wind tunnel by Li and Meroney (1983) with the present CFD simulation along Line-h1. Only the last three meshes (3, 4 and 5) were included since the condition of using EWT in Fluent is that Y^+ in the near-wall region must be kept less than 5. Firstly, it is observed from the experimental data that the tracer gas is mainly transported upwind of the vent. This is caused by the well-known reversed flow on the front edge of the building roof. It is also observed that the Realizable model using the turbulence Schmidt number (Sct) equal to 0.3 (a parameter to be discussed later in this section), tends to successfully capture this relative high concentration in the upwind zone of the vent for the three meshes. Among the meshes presented, mesh 3 represents an acceptable compromise between computing cost and result accuracy. Therefore and based on this analysis, the meshing strategy used in the present study considers high mesh concentration in the near-wall region with a Y^+ near to 5 in order to use the EWT technique.

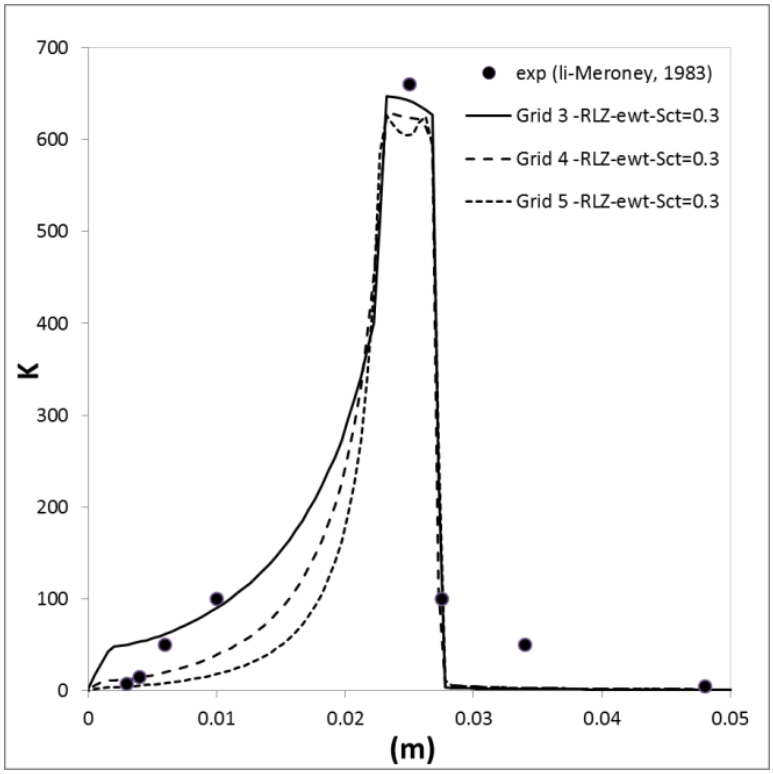

Figure 3.4 – Comparison of K between experimental data and Realizable turbulence model results along Line-h1.

The meshing for the current study is shown in Figure 3.5. Keeping Y^+ less than 5, the mesh size was 1,833,164 cells.

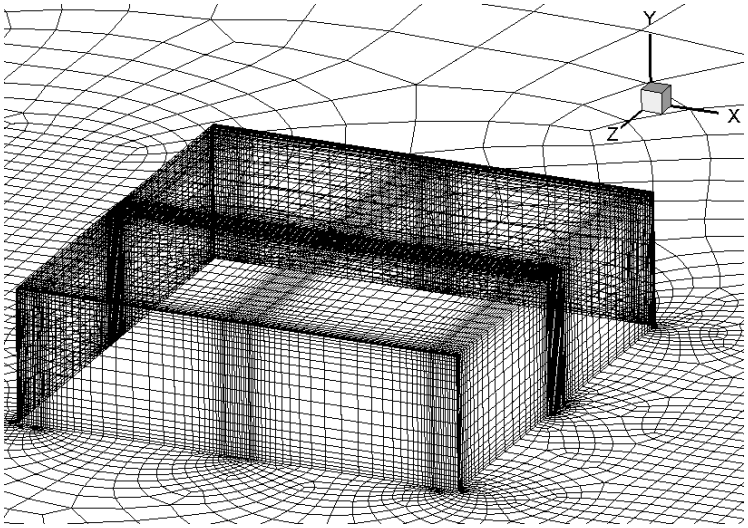

Figure 3.5 – Meshing used for isolated emitting building (1,813,164 cells).

3.2.3 Boundary conditions

An important part of the present study is the numerical validation process which is based on wind tunnel data and CFD comparisons for a selected group of building configurations. In order to minimize the number of uncertainties, CFD boundary conditions are defined as similar as possible to the wind tunnel experimental setup. In others words, CFD simulations try to reproduce the wind tunnel, then all the parameters are adjusted to the wind tunnel scale, which is 1:200. The following is a description of the boundary condition used all along the present study.

The bottom surface (i.e. ground) is a rigid plane with an aerodynamic roughness length y_o=0.0033 m (which corresponds to y_o=0.66 m at full scale). At the outlet, an outflow (zero gradient) condition is specified to generate a fully developed flow. Building walls, top and sides of the domain are modelled as no slip walls. As with the wind tunnel experiment, a power law exponent of 0.31, which corresponds to a light urban terrain (Simiu and Scanlan, 1996), is used for the inlet wind profile and defined as follows:

$$U(y) = 6.3\left(\frac{y}{0.075}\right)^{0.31}$$

The pollutant released from stack is simulated with SF_6 for a particular exhaust momentum ratio, *M*. The dispersion of pollutants is analysed using the normalized dilution concept, which can be explained as follows: if a pollutant is discharged with a certain initial concentration, this concentration will be reduced as the pollutant travels within the atmosphere mixing with clean air. Then, dilution is defined as the ratio between the source concentration and the measured concentration at a specific point in the domain. Consequently, the lower the measured concentration the higher the dilution value will be.

The following formulation, suggested by Wilson (1979), was used to evaluate the normalized dilution, D_N:

$$D_N = \frac{D_r Q}{U_H H^2}$$

where:

$D_r = C_e / C_r$ is the dimensionless concentration coefficient at the coordinate location (named also receptors);
C_e = contaminant mass fraction in exhaust (this study used 10 ppm of SF_6);
C_r = contaminant mass fraction at the coordinate location (ppm);
Q is the flow rate at the exhaust (m^3/s);
U_H is the wind speed at the emitting building height (H). The velocity at the isolated building (b1) height is 6.3m/s.

Figure 3.6 shows the profiles of mean wind speed (a) and turbulence intensity quantities (b) measured in the wind tunnel. These profiles are used to specify the inlet condition in the numerical model. The mean velocity profile was approximated by power law exponent of 0.31, which corresponds to an urban terrain. The velocity at the building b1 height (H = 0.075 m) was U_H = 6.3 m/s.

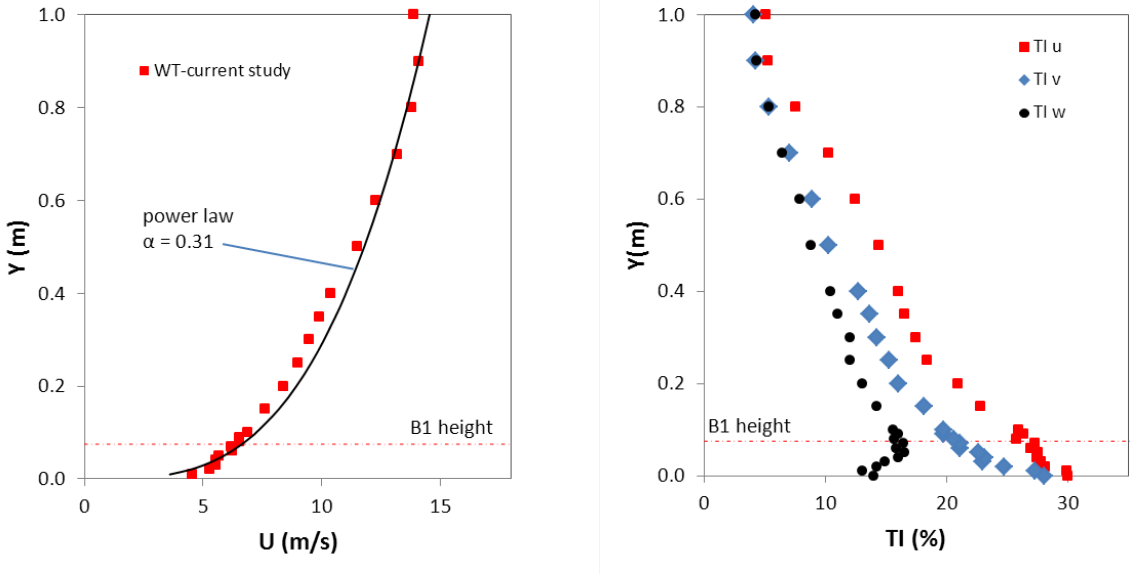

a) **b)**

Figure 3.6 – Atmospheric boundary layer profiles from wind tunnel: a) mean velocity, b) turbulence intensity.

The measured turbulence intensity profiles are converted in a turbulent kinetic energy (k) profile using two options. Option 1: k is calculated from turbulent intensity measurements in the wind tunnel considering the three components of fluctuating velocities $\langle u' \rangle, \langle v' \rangle$ and $\langle w' \rangle$

assuming $\langle u' \rangle = TI_u U/100$; and Option 2: *k* is calculated assuming isotropic turbulence and only the x component, $\langle u' \rangle$, of the measured velocity is used (van Hooff and Blocken, 2010).

Option 1: $k = \frac{1}{2}(\langle u' \rangle^2 + \langle v' \rangle^2 + \langle w' \rangle^2)$

Option 2: $k = \frac{3}{2}\langle u' \rangle^2$

As shown in Figure 3.7, Option 2 presents a relatively high value of *k* in the low level of the boundary layer, as compared with Option 1. The dissipation rate profile (ε) was defined as $\varepsilon = u^{*3}/\kappa y$ where κ is the von Karman constant (0.42) and u* is the friction velocity obtained from the equation $u(y)/u^* = 1/\kappa(\ln(y/y_o)$ with roughness length y_o = 0.0033 m. At the model scale of 1:200, the equivalent full-scale roughness length is 0.66 m, which is at the low end of the expected range for an urban environment (0.5 m < y_o<1.5 m) (Stathopoulos *et al.* 2004). In order to introduce these turbulence parameters as well as the mean wind velocity profile at the inlet boundary of CFD model, a UDF was implemented.

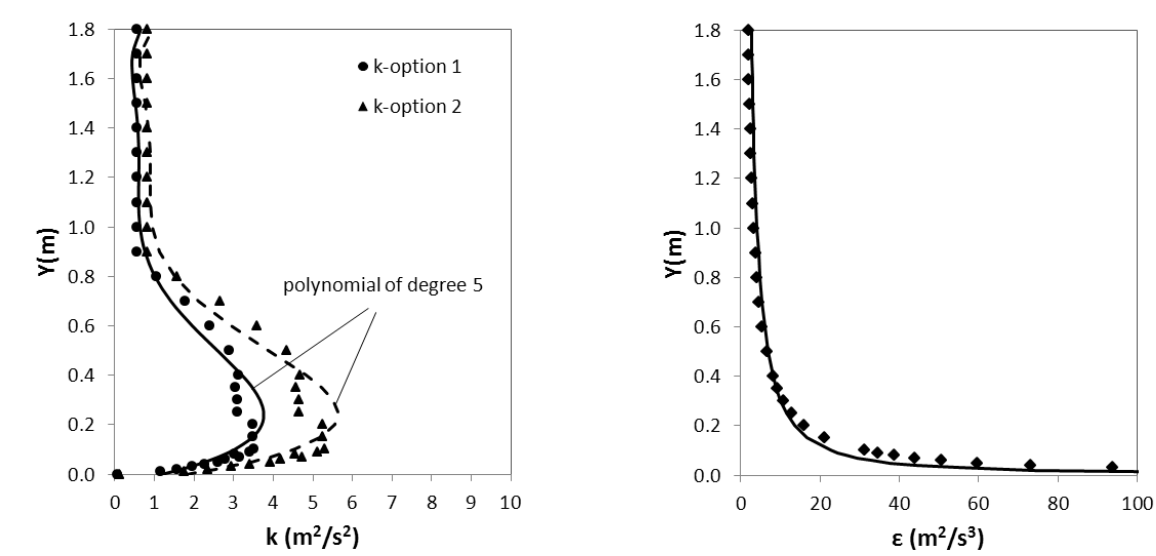

Figure 3.7 – Turbulence kinetic energy and dissipation profiles evaluated from wind tunnel data.

Figure 3.8 shows the impact of using the two different *k* profiles on D_N obtained at the roof center line of a particular building configuration. The case used in this comparison corresponds to a two-building configuration shown in Figure 3.10b. The results show no relevant impact on the dilution values at the roof level. Therefore, Option 1 was used in this study since it provides more physical meaning, as actual fluctuations in all directions are included.

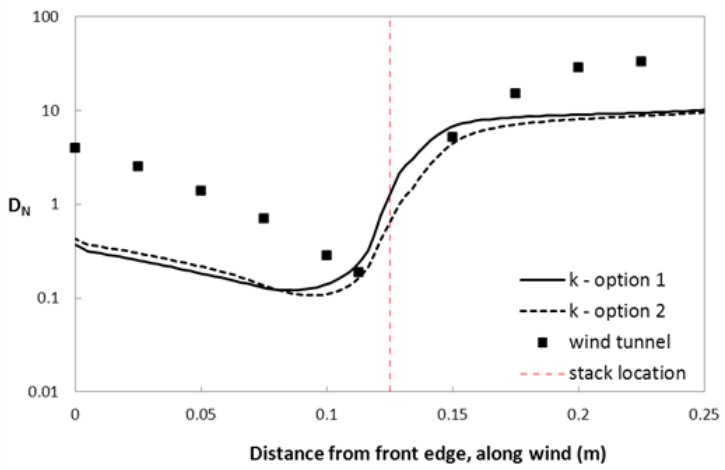

Figure 3.8 – Effect of turbulence kinetic energy profile on D_N at roof level.

The computational domain and boundary conditions are summarized in Figure 3.9.

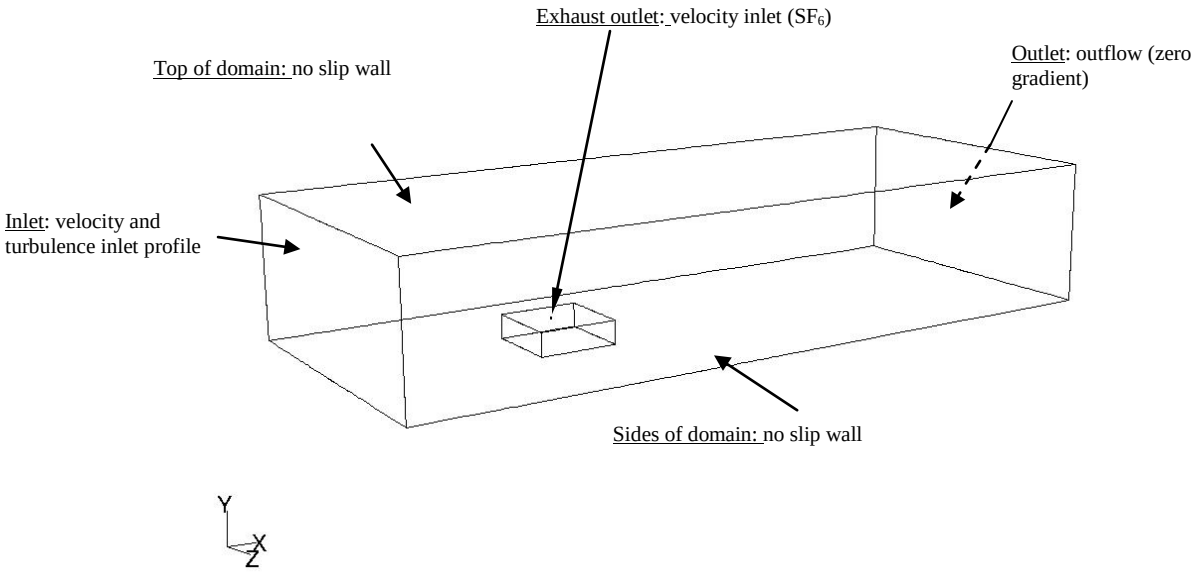

Figure 3.9 – Boundary conditions of CFD model.

3.2.4 Turbulence model

Dispersion simulation at roof level on an isolated emitting and on a two-building configuration (Figure 3.10a and b, respectively) was performed using four different turbulence models, namely: Standard k-ε (SKE), Realizable k-ε (RLZ), Renormalized Group k-ε (RNG) and Reynolds Stress-Model (RSM). The results were compared with experimental data obtained by the authors for an identical configuration.

For all simulations, all transport equations (momentum, energy, turbulence variables and concentration) were discretized using second-order upwind scheme. The SIMPLE algorithm was used for pressure-velocity coupling.

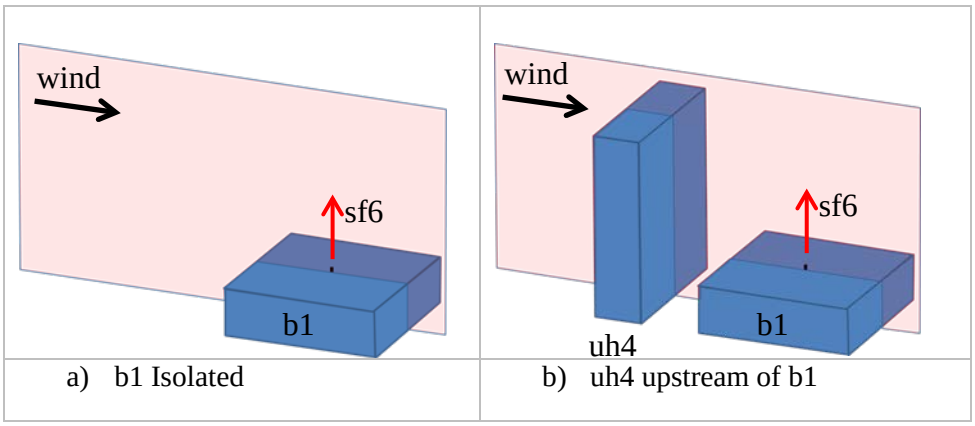

a) b1 Isolated b) uh4 upstream of b1

Figure 3.10 – Schematic representation of isolated and non-isolated cases.

Figure 3.11a shows D_N at roof level for an isolated emitting building with an exhaust stack in the middle of the roof. In general, it is observed that numerical prediction of D_N is underestimated downwind the stack and overestimated upwind the stack compared with experimental data. However, even if D_N is underestimated, an acceptable good trend is observed for SKE, RLZ and RSM models, downwind of the stack region. The region upwind the stack is characterized by a significant D_N overestimation for all turbulence models. It is observed that SKE and RLZ performed very similarly in all the regions and RSM showed an important improvement compared with SKE and RLZ in the upwind region, but still D_N is over-predicted. RNG provided higher D_N values near the stack in the downstream part of the roof (compared with all other models). All cases were obtained using the standard (default value by Fluent) Sct=0.7.

Figure 3.11b shows D_N at the same location described previously, but now there is a building located upstream of the emitting building. The values of D_N obtained by RSM, SKE and RLZ present similar trends in all the regions compared with experimental data and an acceptable good agreement downwind the stack. In the region upwind the stack, D_N is significantly underestimated by all the turbulent models tested. As previously mentioned, RNG provided higher D_N values near the stack in the upstream part of the roof. Again, all cases consider Sct=0.7.

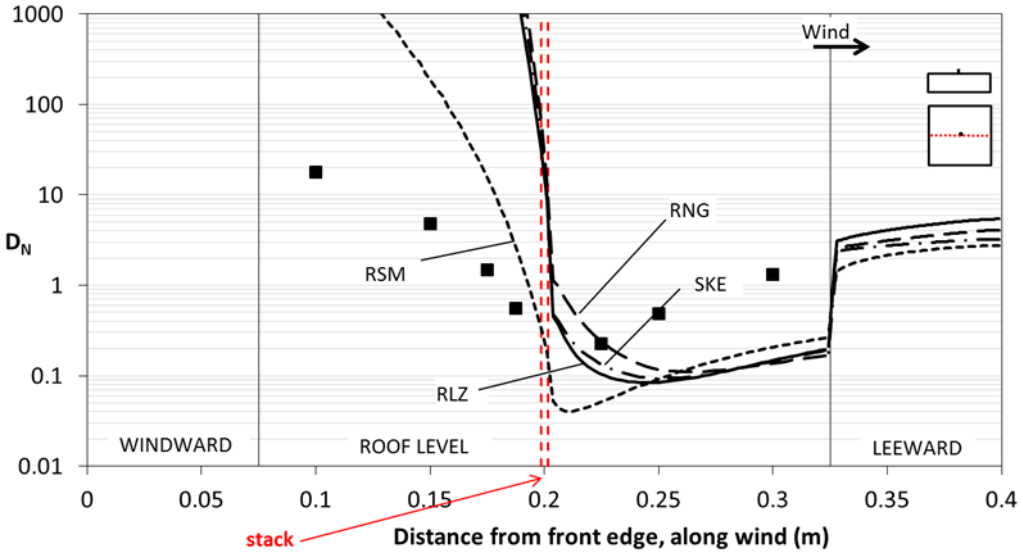

a) Isolated emitting building

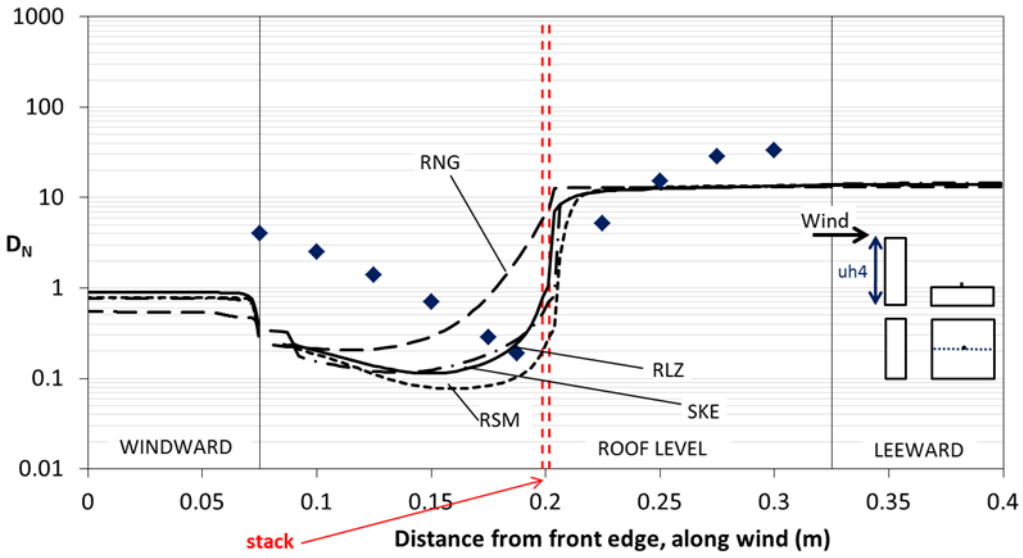

b) Non-isolated building

Figure 3.11 – D_N affected by turbulence model using default Sct value (Sct=0.7).

3.2.5 Schmidt number

Turbulent Schmidt number (Sct) is necessary to solve the transport mass equation in CFD prediction of dispersion with RANS and is defined as the ratio of turbulent viscosity to the turbulent mass diffusivity ($Sct=\nu_t/D_t$). In FLUENT, Sct must be declared as input prior to any calculation or else the default value assumed is 0.7. Past studies have shown the dependence of Sct on simulation of pollutant dispersion and that Sct values between 0.1 and 0.3 have good

agreement with experimental results for tracer experiments involving pollutants around buildings (Tominaga and Stathopoulos, 2007; Blocken *et al.* 2008, Chavez *et al.* 2011). The following is a sensitivity analysis of Sct on D_N for two building configurations: an isolated emitting building and an emitting building with another building located upstream (Figure 3.12).

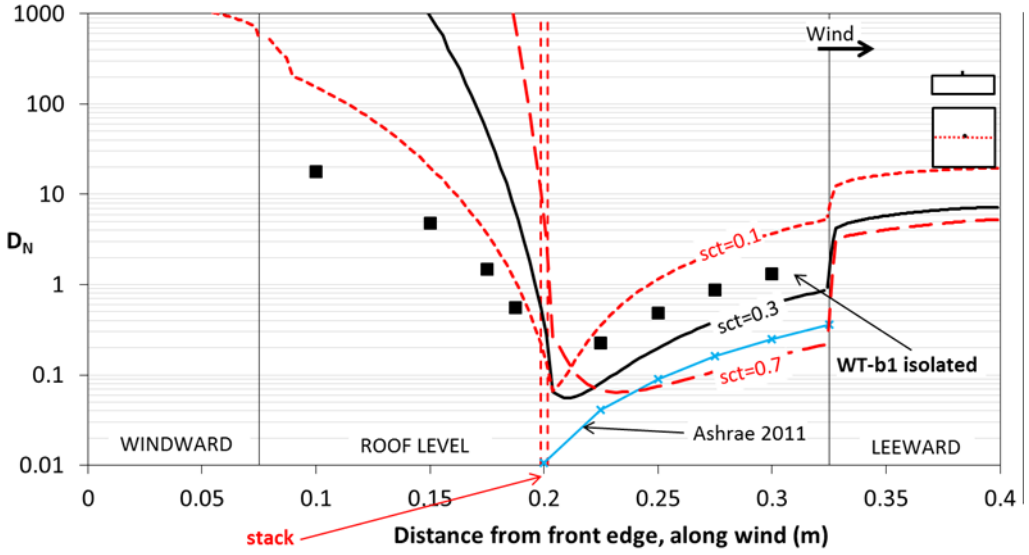

a) Isolated emitting building

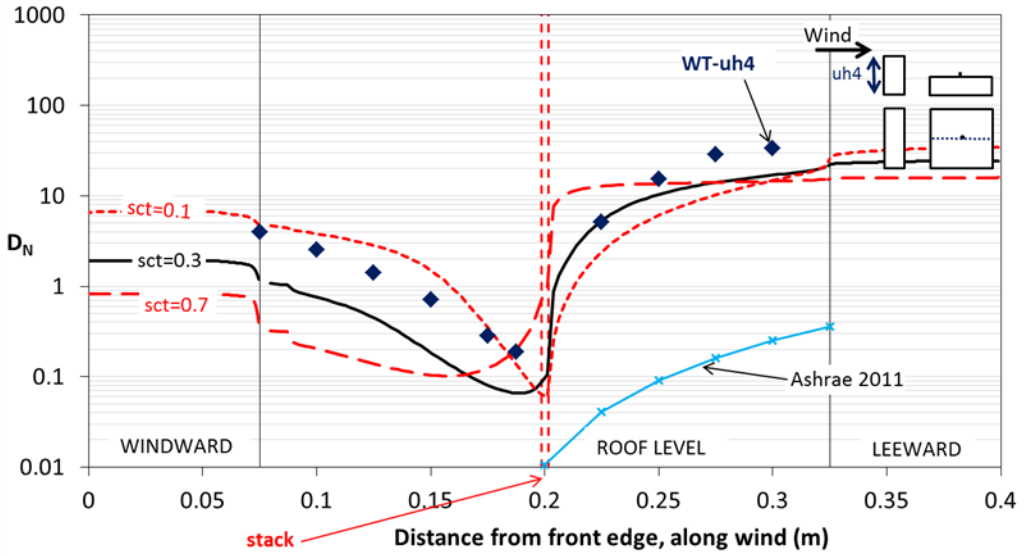

b) Non-isolated emitting building

Figure 3.12 – Effect of Sct on D_N using Realizable turbulence model.

Figure 3.12a shows the effect of Sct on D_N for an isolated emitting building. The results confirm that pollutant dispersion is greatly influenced by the value of Sct in both regions, upwind and downwind, of the stack. In contrast, it can be noted in Figure 3.12b that Sct has a high influence

on the region upwind the stack and very limited influence downwind the stack. This reveals that Sct has dominant effect in regions where pollutants are being spread.

To better visualize the effect of Sct on D_N prediction, iso-contours in all surfaces and an iso-surface of D_N=1 have been plotted in Figures 3.13 and 3.14. The iso-surface D_N=1 permits to visualize the tridimensional behaviour of the plume for different building configuration. In both figures, it is clearly observed that a lower Sct value (0.1) produces a predominant mass diffusivity leading to a plume spreading in all directions with a reduced diffusion along the flow. Then, as Sct increases, the transport mechanism changes and the plume is progressively advected by the computed dominant flow against reduced mass diffusion. Sct influences the mass transport mechanism and not the fluid dynamics (Di Sabatino *et al.* 2007). The computed flow, for both cases, is plotted in terms of streamlines in Figure 3.15. As shown in this comparison, Sct has a large influence on dispersion and it is difficult to generalize a particular Sct in CFD due to its high case-dependence characteristic. However, for the forthcoming simulations, Sct is fixed at 0.3 since this value represents a good compromise between an artificial numerical calibration and physical meaning.

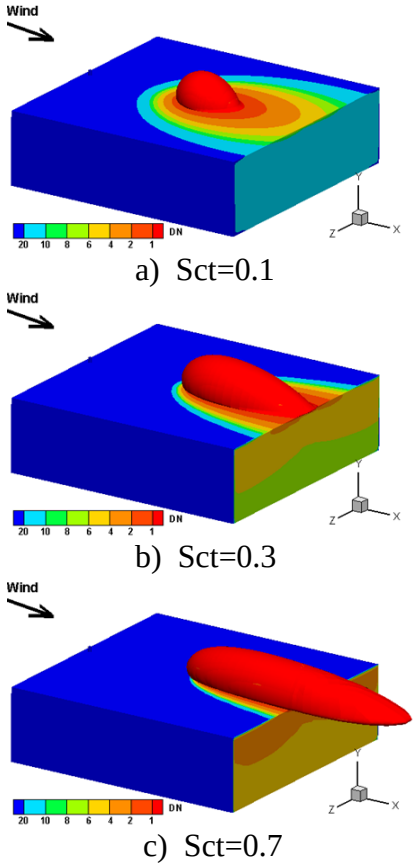

a) Sct=0.1

b) Sct=0.3

c) Sct=0.7

Figure 3.13 – Dilution contours (b1 isolated) and isosurface of D_N=1 for three different Sct.

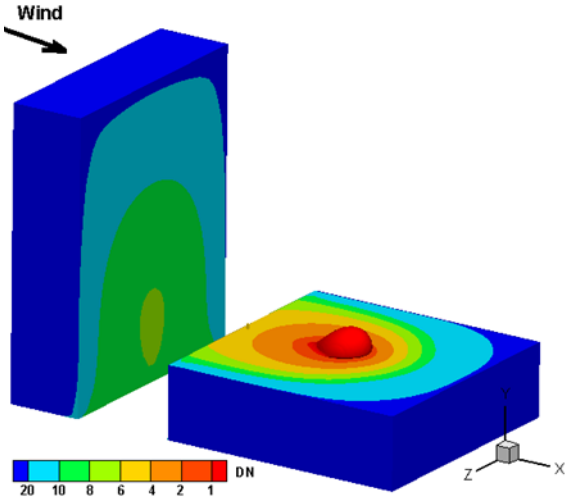

a) Sct=0.1

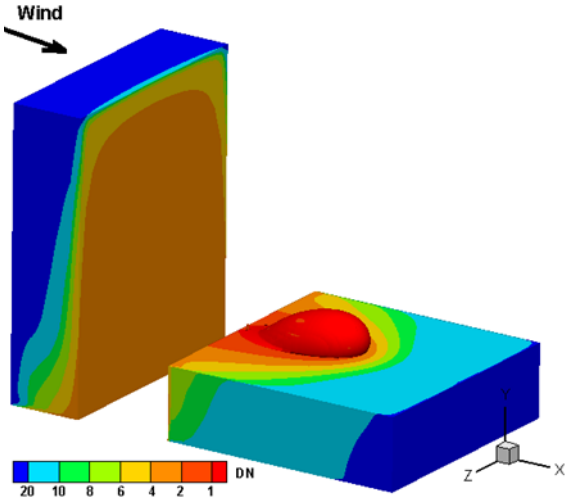

b) Sct=0.3

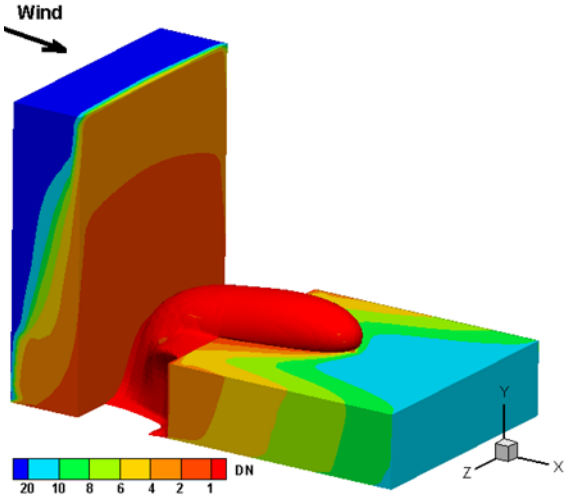

c) Sct=0.7

Figure 3.14 – Dilution contours (uh4 upstream of b1) and isosurface of D_N=1 for three different Sct.

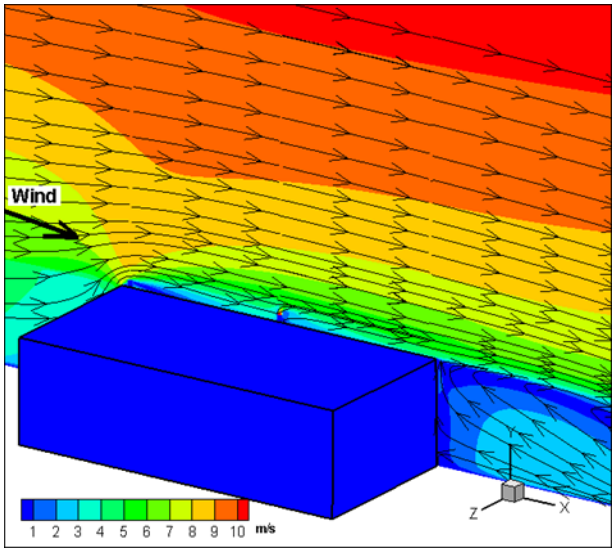

a) b1 isolated

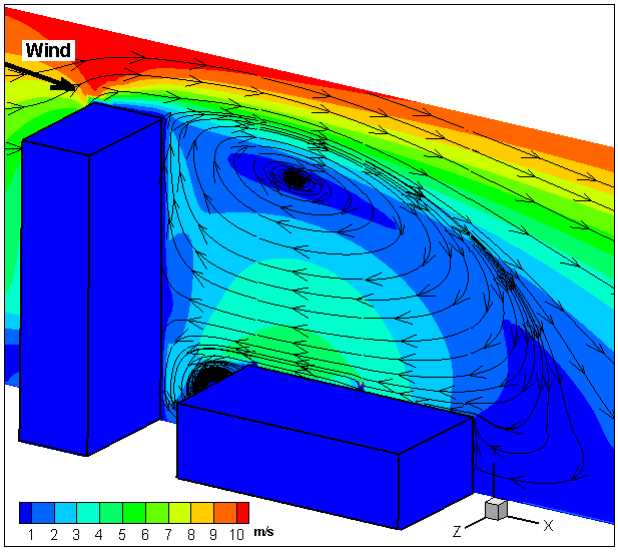

b) uh4 upstream of b1

Figure 3.15 – Stream lines and iso-contours of the velocity magnitude in the middle elevation plane.

3.2.6 Convergence criterion

The convergence criterion is generally based on the residuals of equations which serve to designate how far the current solution is from the exact solution (Franke *et al.* 2007). Knowing that the exact solution is obtained after an infinite number of iterations, the convergence criterion becomes then the stopping criterion of the iterative process. The convergence criterion is a critical parameter that should be defined before and monitored during any CFD calculation. Unfortunately, there is no clear consensus in the literature about the level of iterative convergence, apart that a typical industrial stopping criterion is 10^{-3}. For research purposes, it is suggested to decrease it to 10^{-5} (Ramponi and Blocken, 2012; Franke *et al.* 2007). The current section explores the influence of residual definition for D_N prediction for an isolated and a non-isolated building configuration.

Figure 3.16a shows clearly that any reduction of the convergence criterion from 10^{-5} shows almost no changes in the final solution. This means that keeping the standard criterion at 10^{-5} is sufficient for a converged solution for the case of an isolated building. On the other hand, Figure 3.16b, which corresponds to the two-building configuration, shows that convergence criterion reduction has an important effect on the final D_N value, particularly in the upwind of the stack region. Figure 3.17 shows that reducing the convergence criterion from 10^{-5} to $0.9x10^{-5}$ by adding close to 800 extra iterations, D_N varies by more than 500% from the previous value at the specific location x = 0.1m. A further reduction of the convergence criterion demonstrates that to obtain two consecutive variations of D_N by about 7%, a residual equal to $0.4x10^{-5}$ is required. The associated computational cost for reducing the convergence criterion from 10^{-5} to $0.4x10^{-5}$ is reflected on the 8,026 extra iterations needed to reach this level.

In conclusion, in order to limit potential source of error on D_N prediction from not having enough iterations, the convergence criterion was fixed at $0.4x10^{-5}$, i.e. lower than the standard value of $1.0x10^{-5}$, for all the equations. However, for all the non-isolated building cases examined in the present study, about 27,000 iterations are sufficient to reach this level.

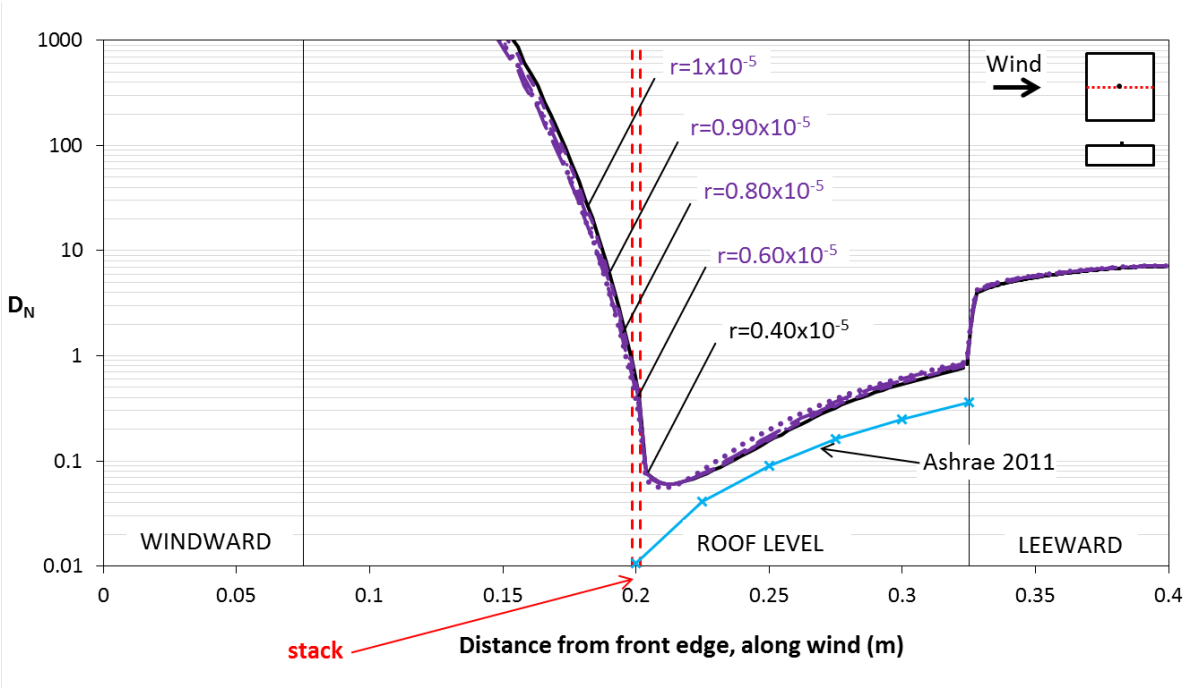

a) Isolated emitting building

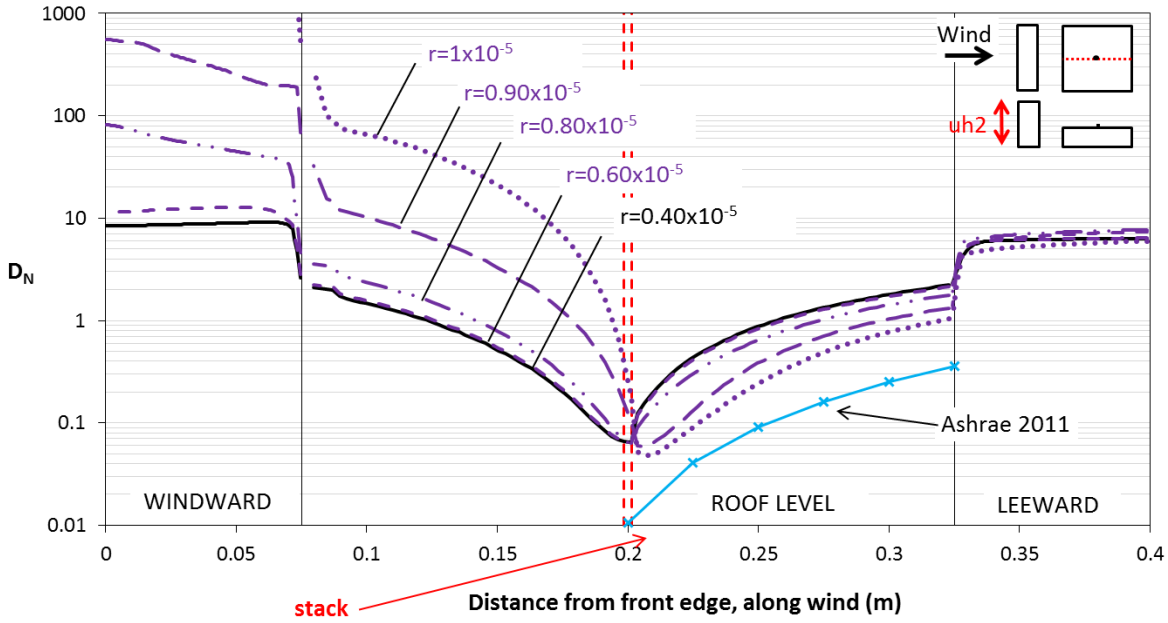

b) Building upstream is twice the height of the emitting building

Figure 3.16 – Variation of D_N for different residual criteria.

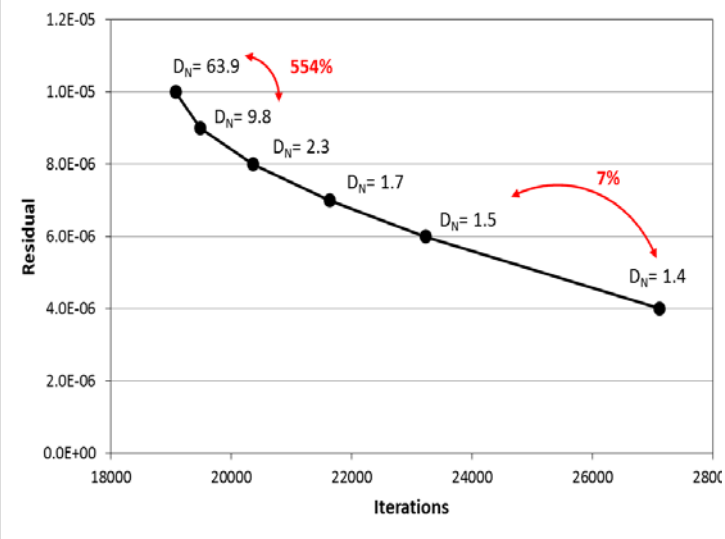

	iterations
Residual = 1 x 10^{-5}	19077
Residual = 0.9x 10^{-5}	19848
Residual = 0.8x 10^{-5}	20362
Residual = 0.6x 10^{-5}	23223
Residual = 0.4x 10^{-5}	27103

Figure 3.17 – D_N for different number of iterations when the upstream building is twice the height of the emitting building.

3.2.7 Unsteady approach

Flows within urban areas are highly turbulent and this causes pollutant mixing and rapid dilution in the near field from the source. The existence of complex vortical structures around buildings is the main difficulty to predict accurately pollutant concentrations. The most used approach for turbulent flow simulation is the set of Reynolds-Averaged Navier-Stokes (RANS) equations. However, numerous publications confirm that inaccuracies for dispersion prediction, especially in the near-field of an emitting building, are detected due to the RANS inherent incapability of reproducing flow unsteadiness in detached regions (Chavez *et al.* 2012). To address this issue – while keeping low computational cost – some effort was made to use the unsteady RANS approach (URANS) with unsatisfactory results. Indeed URANS performance problems can be found in the literature, which suggests that further investigation is needed for complex flow conditions (Iaccarino *et al.* 2003). For this reason, RANS is being replaced by the unsteady approach LES. The attractiveness of LES lies on the fact that only small scales of turbulence are modeled, while large turbulent structures are directly solved. The computational cost, however, is extremely high.

Using the same meshing for all cases and with no particular fluctuating velocity algorithm at the inlet for the unsteady approaches, Figure 3.18 shows normalized dilution comparison for RANS, URANS (both using the RLZ turbulence model) and LES. The results correspond to a three-building configuration identified as uh2dh4 (Table 4 in section 4.1). It is noted that URANS shows identical results with RANS and both underestimate the dilution at the roof level. On the other hand, LES seems to follow the trend of the experimental data at the roof level – where the turbulence activity is very high – but still the results are not conclusive, evidencing that more computing time is needed. It is important to note that the experimental data correspond to the average of 2 min (real time) sampling. By contrast, the presented LES values correspond to an average of 5 second simulation using a 10^{-3} second time step (about 3 days of calculation using 4 parallel processors). The cost associated with LES simulation was close to 100 times greater than

that incurred with the RANS, as declared by Cheng *et al.* (2003), when using same computational power for both approaches.

Even if the accuracy of LES is not completely evaluated in this report, its use for parametric studies is not recommended. The computing effort necessary for a good LES simulation is too high compared with RANS and this without any substantial accuracy improvement, at least for the current case. Consequently, it was decided to apply only the RANS approach for the present pollution dispersion. In the following Chapter, several comparisons with experimental data will be carried out in order to evaluate dispersion prediction using RANS for isolated and several non-isolated building configurations.

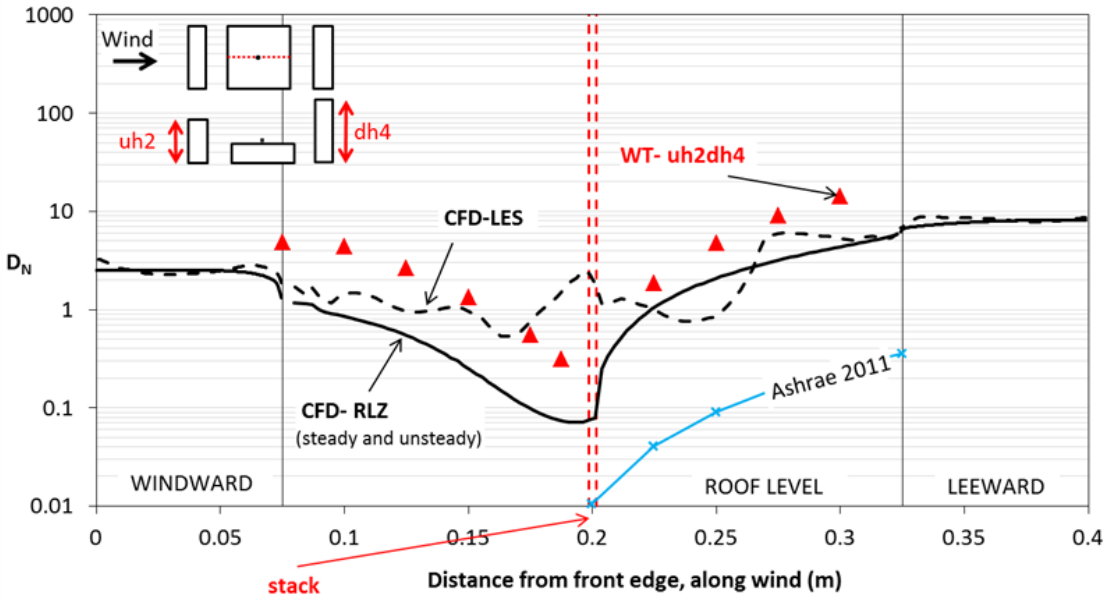

Figure 3.18 – Variation of D_N at roof level of an emitting building using steady and unsteady RANS (realizable turbulence model) and LES approaches.

3.3 Wind tunnel experiments

The wind tunnel experiments were carried out in the open circuit variable height boundary layer wind tunnel at Concordia University. Its dimensions are 1.8 m by 1.8 m in section and 12.2 m in length. The building models tested were made of timber on a 1:200 scale. A tracer gas technique was used to investigate the concentration (or dilution) pattern of gases spread in the atmosphere from the exhaust. The technique consists of injecting SF_6 from the exhaust and then detecting the concentration at various specific locations (receptors). A multi-syringe pump was used to collect the gas samples to determine the concentration at various rooftop receptors of the emitting building b1, with a sampling time of 2 minutes. More details concerning the experiments setup can be found in the first part of the current research project (Stathopoulos *et al.* 2014).

4. EVALUATION OF RANS MODELS FOR POLLUTANT DISPERSION

4.1 Cases studied

For all cases a single wind direction perpendicular to the building face was considered. Dilution concentration measurements were carried out using receptors located centrally on the rooftop of b1 (emitting building), as shown in Figure 4.1a. In this study only one stack location was used which is in the middle of the roof. For other cases, i,e. stack in the front edge, additional comparisons between wind tunnel and CFD can be found in Appendix A. Concerning the adjacent buildings, three scenarios were analysed: the effect of an upstream building, the effect of a downstream building and the effect of both upstream and downstream buildings (Figure 4.1b, c and d). For each configuration, four different heights for the adjacent building were considered. The specific dimensions of each building are detailed in Tables 2, 3 and 4. Thus, considering a single stack location, 12 cases were analysed. In all cases, the adjacent building, either upstream or downstream, is located 0.1 m away from the emitting building.

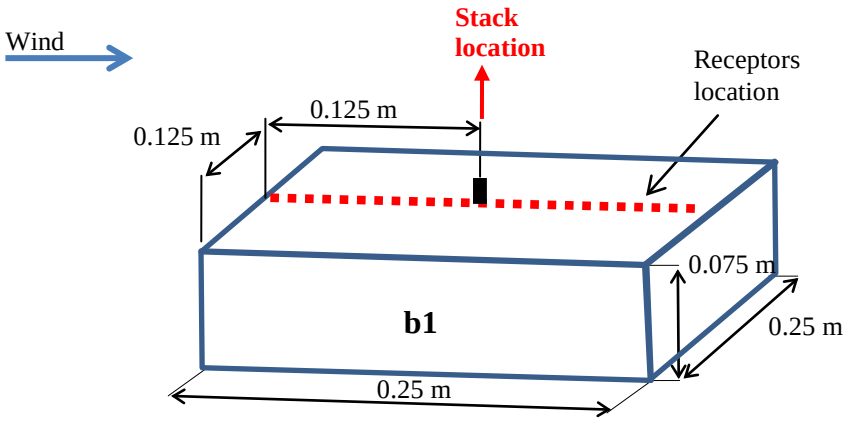

a) Emitting building (b1)

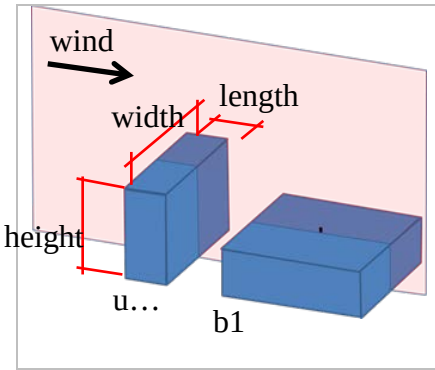

b) b1 with an upstream (u…) building

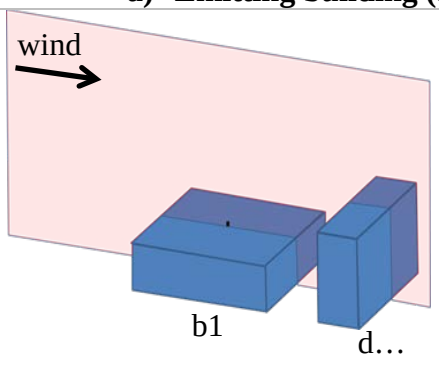

c) b1 with a downstream (d...) building

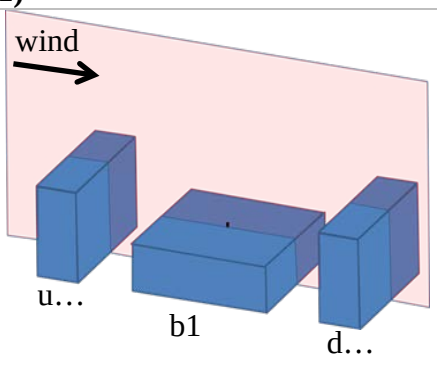

d) b1 with both, upstream (u…) and downstream (d…) buildings

Figure 4.1 – Emitting building and three configurations of adjacent buildings.

Table 2. Dimension of buildings placed upstream of b1.

case	case	Height (m)	Length (m)	Width (m)
1	uh1	0.075	0.075	0.25
2**	uh2	0.15	0.075	0.25
3	uh3	0.225	0.075	0.25
4**	uh4	0.3	0.075	0.25

** wind tunnel data available

Table 3. Dimensions of buildings placed downstream of b1.

case	case	Height (m)	Length (m)	Width (m)
5	dh1	0.075	0.075	0.25
6**	dh2	0.15	0.075	0.25
7	dh3	0.225	0.075	0.25
8**	dh4	0.3	0.075	0.25

** wind tunnel data available

Table 4. Dimensions of buildings located upstream and downstream of b1.

case	case	Height of the upstream building (m)	Height of the downstream building (m)	Length (m)	Width (m)
9	uh1dh4	uh1=0.075	dh4 = 0.3	0.075	0.25
10**	uh2dh4	uh2=0.15	dh4 = 0.3	0.075	0.25
11	uh3dh4	uh3=0.225	dh4 = 0.3	0.075	0.25
12	uh4dh4	uh4=0.3	dh4 = 0.3	0.075	0.25

** wind tunnel data available

4.2 Wind tunnel visualization

Real-world observations and thorough visualization tests can facilitate the understanding of complex flow behaviour and help the conceptualization of physical process as, for example, in the case of dispersion of pollutant around buildings. The wind tunnel visualization via smoke release from the exhaust stack model permits to define the zones of interest and to optimize receptor locations for further analysis. Capturing the actual physics that governs the dispersion of pollutant can be used as a reference for qualitative validation of dispersion prediction obtained by CFD simulations.

Figure 4.2 shows corresponding snapshots for the most representative configurations on dispersion problem: an isolated emitting building and the effect of a building placed upstream and of a building placed downstream of the emitting building.

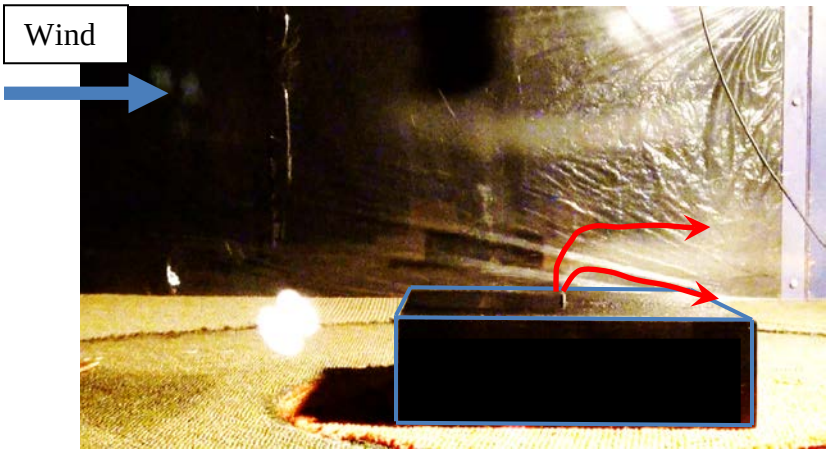

a) Isolated building

The smoke is dragged downstream by the wind.

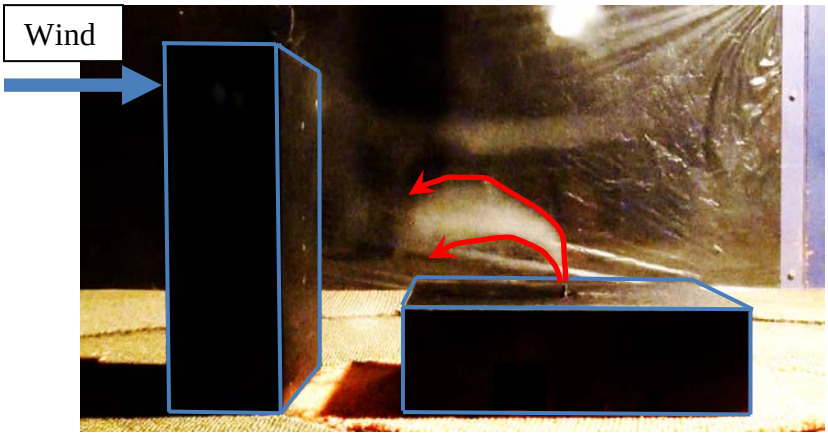

b) Effect of an upstream building

The smoke is trapped in the recirculation zone of the upstream building wake and dragged in the opposite direction of the mean wind stream.

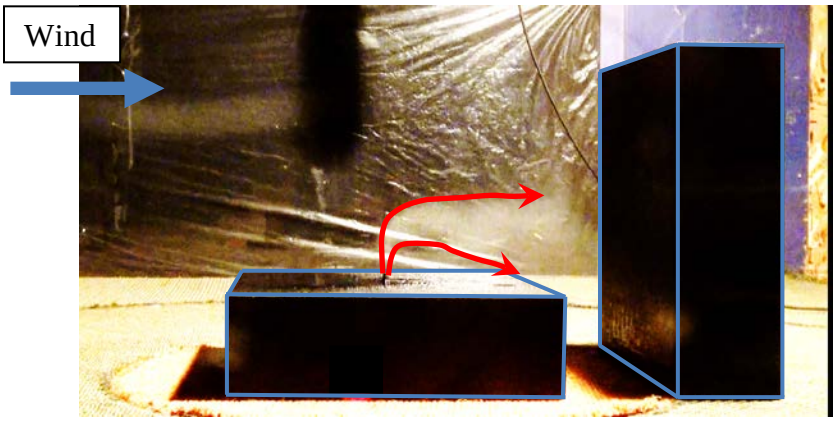

c) Effect of a building placed downstream

A part of the smoke is trapped in the lower part between the two buildings.

Figure 4.2 – Wind tunnel visualization test of adjacent buildings effect.

4.3 Effect of an adjacent building: general comparisons

One of the advantages of CFD simulations is the possibility to obtain a solution in the complete domain. Figure 4.3 shows the contour lines of D_N in the middle vertical plane for the cases shown previously, plus for a three-building configuration. It is important to mention that the D_N plotting range was arbitrarily limited from 0.1 to 30 to better visualize the dilution variations.

Firstly, general views of the computational results show a good qualitative agreement with the wind tunnel visualization test. The isolated building case (Figure 4.3a) shows the usual plume behaviour used for pollutant dispersion modelling; the stack plume is dragged downstream by the wind reducing its concentration by mixing with the atmospheric clean air.

Significant changes in plume behaviour and, consequently, on the D_N field can be noted when a taller building is placed upstream of the emitting building (Figure 4.3b). In this case an upwind displacement of the plume is observed, caused by the swirl in the wake of the upstream building. Since the plume is dragged towards the upstream building, the pollutants tend to pollute the complete leeward façade of the same upstream building. It is observed that complete roof and windward wall of the emitting building is also affected by high pollutant concentration (low D_N values).

The effect of a downstream building is shown in Figure 4.3c. It is noted that D_N does not change significantly along the wind direction; however important changes are noticed across wind direction, this is on the dilution contours at roof level of b1. The spanwise distribution of D_N changes significantly compared with the isolated building case when a downstream building is added in the building layout.

Figure 4.3d shows the D_N distribution for a three building configuration. In this case it is noted that pollutants reach the leeward and windward walls of both buildings adjacent to the emitting building.

This comparative view of different building configuration demonstrates that significant differences can be obtained on the D_N field when the building layout increases its complexity from isolated to multiple-building configuration. More details about the D_N fields and streamlines for different configurations can be found in Appendices B and C respectively.

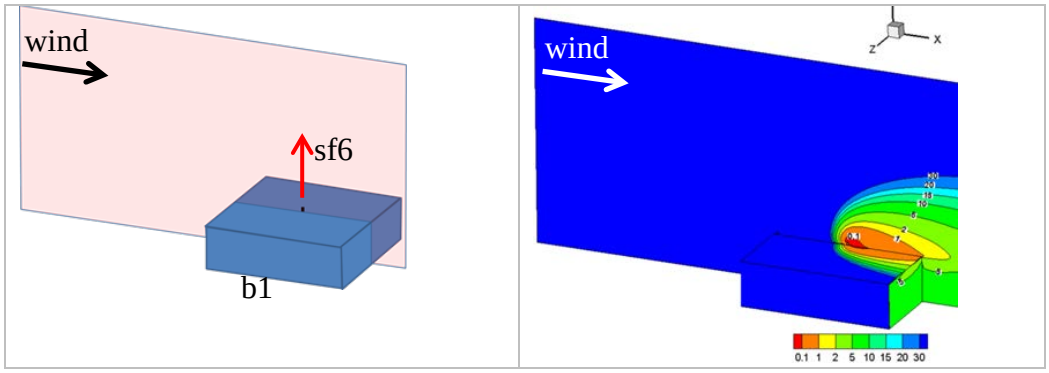

a) An isolated emitting building

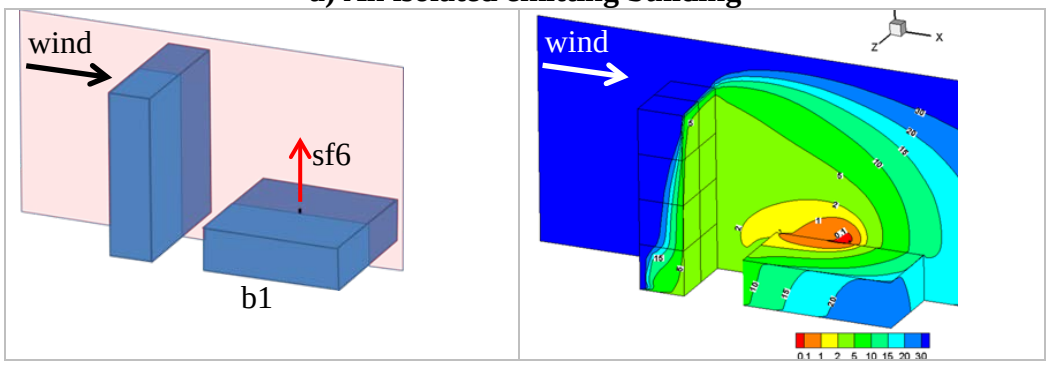

b) A tall building located upstream of an emitting building

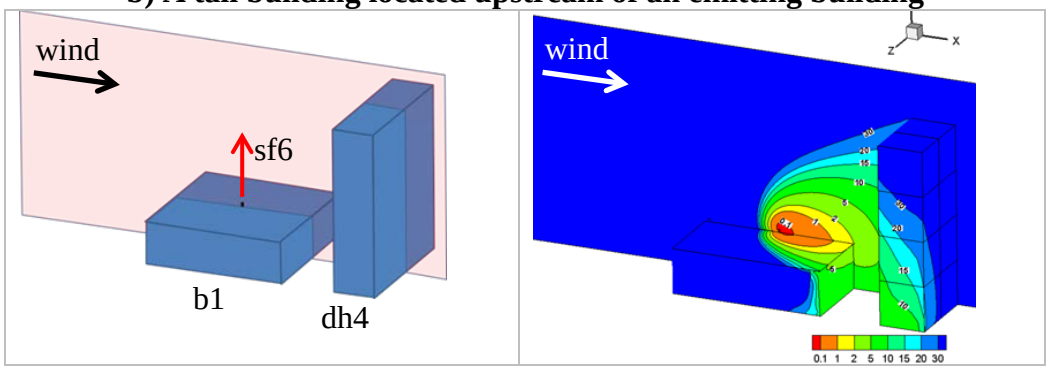

c) A tall building located downstream of an emitting building

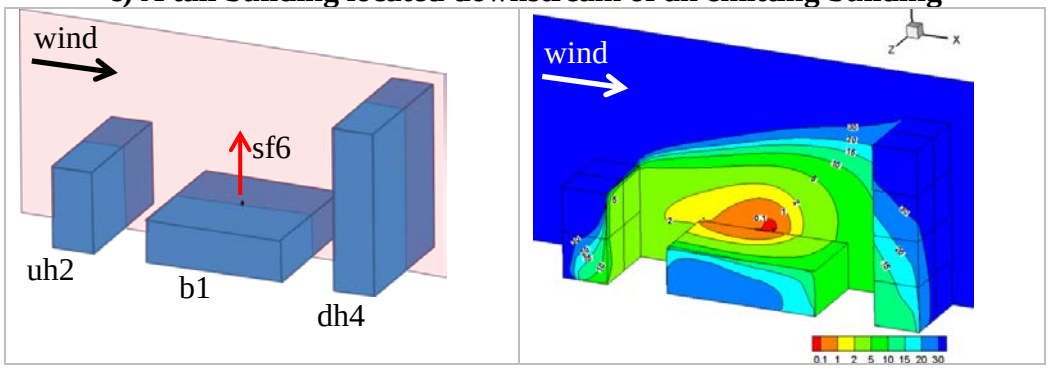

d) An emitting building located between two buildings

Figure 4.3 – D_N in the middle elevation plane for different configurations.

4.4 Validation of CFD model: comparison with wind tunnel and ASHRAE 2011

4.4.1 Isolated emitting building

Figure 4.4 shows the comparison between CFD and experimental data for D_N prediction for an isolated emitting building. From the wind tunnel data, it is observed that D_N increases almost linearly for locations away from the stack in the wind stream direction. This phenomenon is expected since wind naturally tends to blow away pollutants and decrease concentration (increase dilution) from the source. It is noted that CFD follows the trend of wind tunnel data in the region downwind the stack very well; however the computed D_N values are underestimated by a constant factor. The underestimation can be probably associated to the inherent limitations of RANS to capture unsteadiness in a high turbulent regime. High turbulence is characterized by a high mixing rate, which promotes dilution and this is exactly what is underestimated in the present CFD results. Additional comparisons when the stack is located in the front edge of the building have shown similar characteristics, i.e. an acceptable trend agreement and an underestimation of D_N values from CFD predictions (Appendix A). For the region upwind the stack, CFD results over predict D_N significantly, as has been already pointed out in the turbulent model section. ASHRAE 2011 shows good trend but underestimates dilution values.

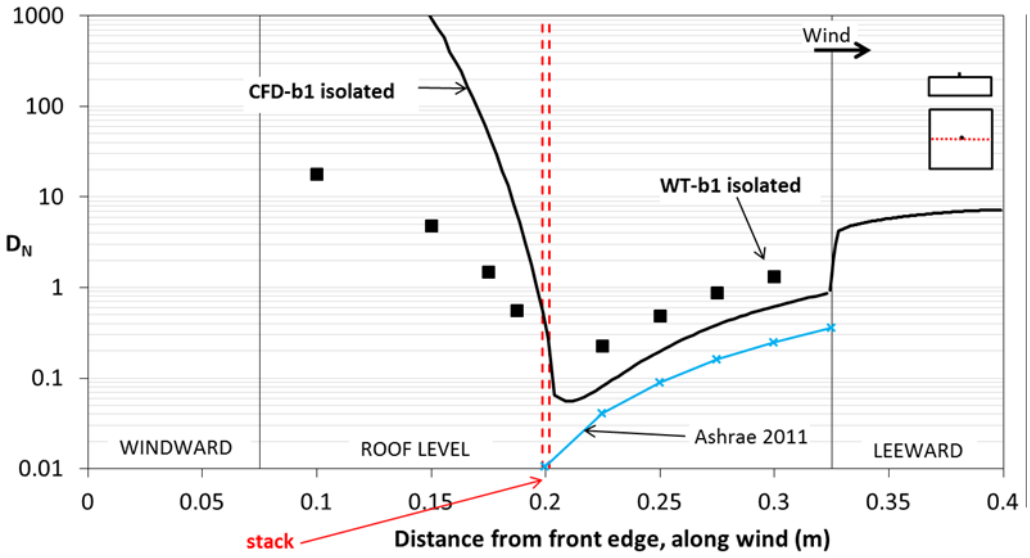

Figure 4.4 – D_N for an isolated emitting building when stack is in the middle of the roof.

4.4.2 A building located upstream of an emitting building

Figure 4.5 shows comparisons of D_N predictions when a building is located upstream of the emitting building with a stack located in the middle of the roof. Building uh4 is an upstream building having four times the height of the emitting building (b1) and uh2 is two times higher than b1. In general, the experimental data show that D_N at the roof level of b1 tends to increase

from the source in both directions upwind and downwind the stack. This behaviour is logical in the sense that depending on the size of the recirculation zone within the wake of the upstream building, the plume can be dragged in the upwind or downwind direction or a combination of both.

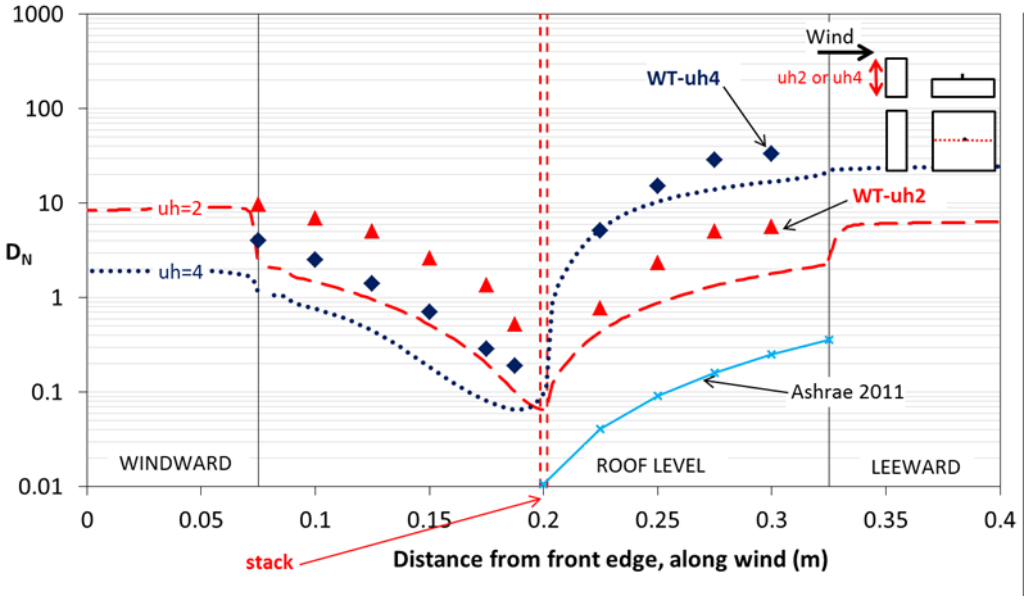

Figure 4.5 – D_N when a building is located upstream of an emitting building with the stack in the middle of the roof.

The wind tunnel data show that uh4 causes low dilution upwind the stack compared with uh2. For the region downwind of the stack the inverse is noted, that is dilutions for uh4 are higher compared with uh2. The phenomenon can be explained by saying that for the uh2 case, the recirculation zone partially traps the plume from the stack leaving some pollutant to spread downwind the stack. When the height of the upstream building increases, the recirculation region increases and more pollutants are carried toward the leeward wall of the upstream building; consequently, fewer pollutants are spread downwind. D_N values clearly depend on the case, but it can be said that for all cases the conservation of mass is respected. The recirculation zone for every case can be visualized in the Appendices B (D_N iso-contours) and C (streamlines). The numerical results show generally good trend compared with experimental data for both configurations. Therefore, it can be said that CFD reproduces the physics of the problem well. However, as previously observed, the numerical results show a constant underestimation of D_N values, particularly in the upwind region for the uh2 case.

Additional comparisons between wind tunnel data and CFD when the stack is located in the front edge of the roof are presented in Appendix A. Those results confirm that in general, numerical solutions reproduce the physics of the problem well with a slight underestimation of D_N along the roof of the emitting building.

4.4.3 A building located downstream of an emitting building

Figure 4.6 shows the comparison of CFD and wind tunnel data when a building, two times taller than the emitting building, is located downstream of this emitting building, with a stack located in the middle of the roof. The experimental data show a very similar behaviour compared with the isolated emitting building case (Figure 4.4). In general, it is observed that D_N field is slightly affected along the wind stream direction when a downstream building is included in the layout. As for previous cases, the comparison between wind tunnel data and CFD shows a good agreement in terms of trend, but also a small underestimation in the region downstream the stack. An additional comparison when the stack is located in the front edge of the emitting building can be found in Appendix A.

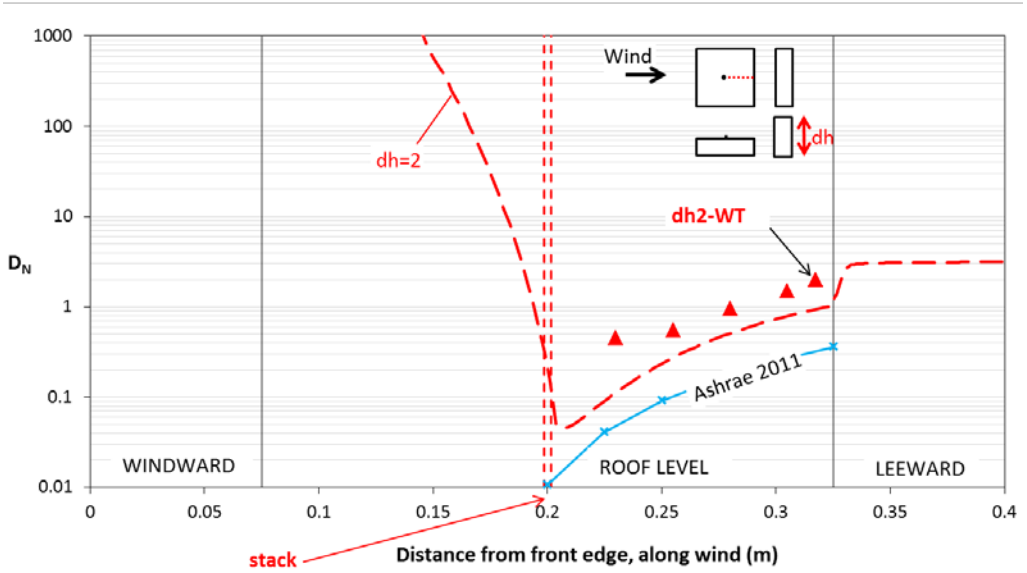

Figure 4.6 – D_N when a building is located downstream of an emitting building with the stack in the middle of the roof.

4.4.4 An emitting building placed between two buildings

Figure 4.7 compares D_N predictions for a three-building configuration. In this case, the emitting building stands between a building which is two times taller, located upstream (uh2) and a building which is four times taller, located downstream (dh4). In general, it is observed that D_N increases in both directions upwind and downwind from the stack, similar to the upstream building case seen previously. Comparing Figure 4.5 with Figure 4.7, it is noted that the combination of two adjacent buildings affects the D_N distribution at the roof level of the emitting building significantly. In fact, it is noted that the addition of dh4 decreases D_N in the upwind region and increases D_N in the downwind region compared to the case when uh2 is alone. For more details, the D_N iso-contours can be visualized in Appendix B. Again, CFD presents a good trend agreement with an underestimation of D_N, particularly in the upwind part of the roof.

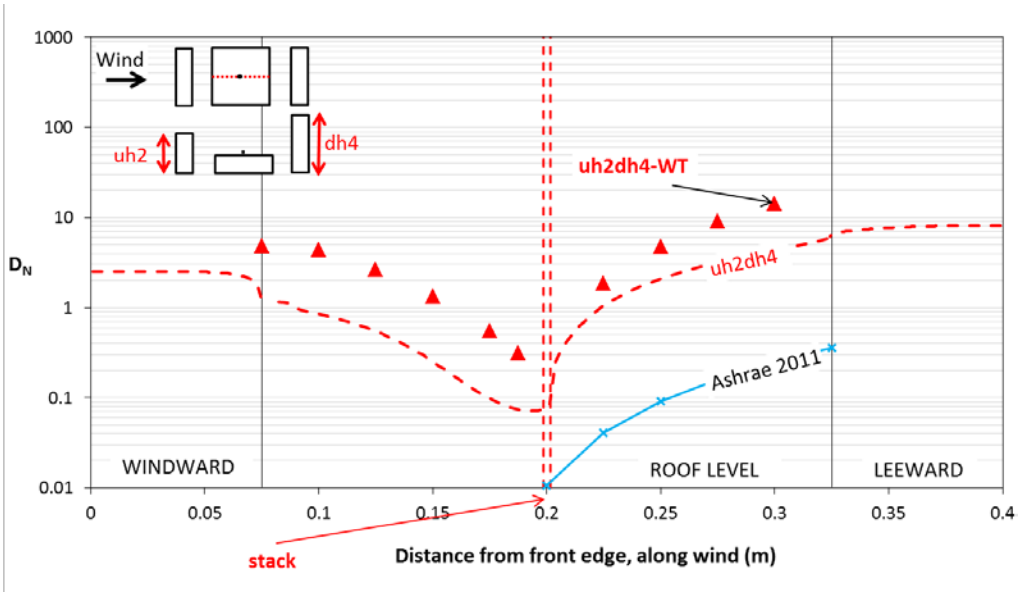

Figure 4.7 – D_N when an emitting building is located between two buildings.

4.5 Effect of an adjacent building: example of a parametric analysis

This sub-section discusses briefly the potential of performing a parametric study of geometric variations on a building layout using a CFD approach. This analysis has taken the form of a parametric study since a single parameter, in this case the height of an adjacent building, was varied keeping all other variables constant. The objective is to detect the range of influence of such parameter on the normalized dilution at a defined location, for instance, the roof level of the emitting building. After plotting various cases, the effect of height is established and useful observations are produced for better understanding the transport dynamics of pollutants around buildings.

Figure 4.8 shows the effect of height of an adjacent building located upstream (a) and downstream (b) of an emitting building. It may be noted that uh=1, 2, 3, 4 and dh=1, 2, 3, 4 are the corresponding height of the adjacent building when it has equal, two, three and four times the height of the emitting building. The gradual growth of the recirculation zone in the wake of the upstream building, as the height of the upstream building increases, causes greater dilution values downstream the stack and a rapid drop in dilution upstream the stack. To visualize the effect of the upstream building height in the complete vertical middle and horizontal plane, dilution contours and streamlines can be viewed in Appendices B and C respectively. Dilution contours shown in Appendix B reveal that parts of the pollutants are dragged upwind toward the leeward wall of the upstream building. Appendix C shows the streamlines for almost all cases, which are useful to understand the plume behaviour for each case. It is noted that uh=4 has an extended wake zone with secondary vortices behind the two buildings in the vertical and horizontal plane compared with uh=2. As a consequence, the plume for uh=2 case is governed by a combination of upwind and downwind flow. In contrast, the plume for uh=4 is almost completely dominated by upwind flow. This explains the dilution behaviour detailed previously

for the upstream building configuration. This observation confirms exactly the conclusion produced in the companion report (Stathopoulos *et al.* 2014).

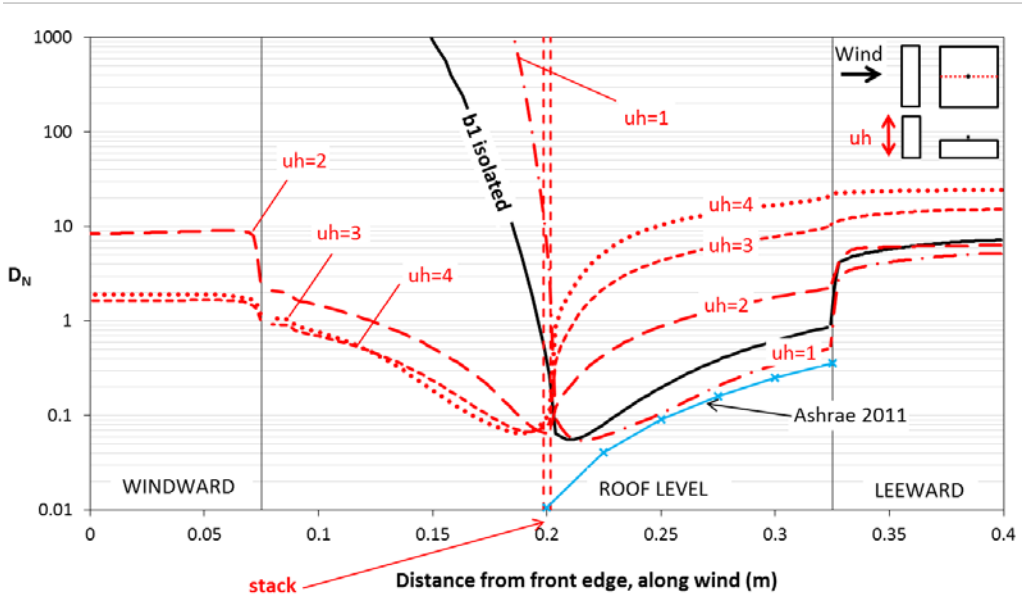

a) Effect of the upstream building height

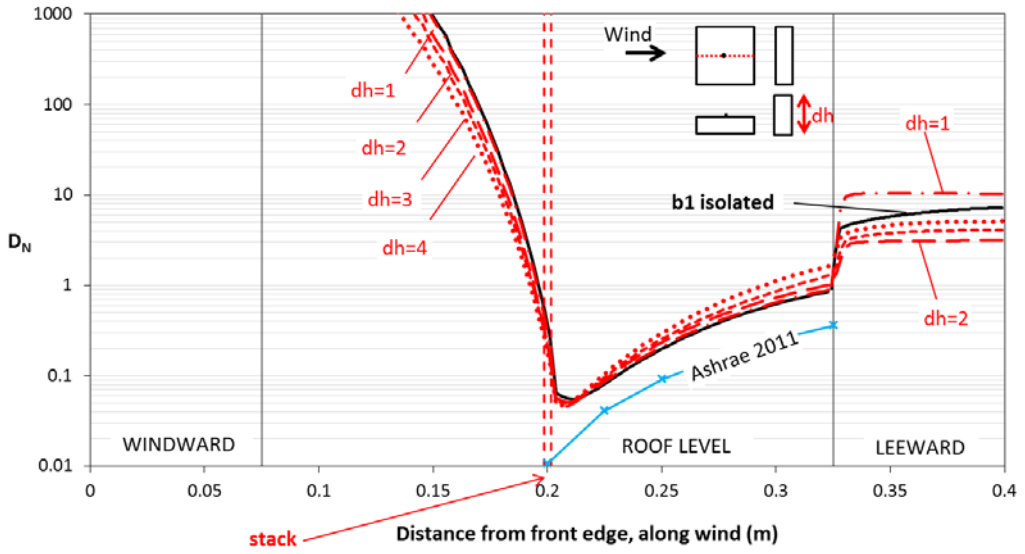

b) Effect of the downstream building height

Figure 4.8 – D_N for two different non-isolated building configurations.

5. CONCLUSION

The present report establishes a reliable method to study the effect of adjacent buildings on the dispersion of effluents using the Computational Fluid Dynamics (CFD) approach. The numerical approach was evaluated by systematic comparison with wind tunnel results obtained previously by the authors (Stathopoulos *et al.* 2014). All the numerical results were presented in terms of normalised dilution, iso-contours and streamlines. This detailed information is crucial for better understanding pollution aerodynamics in urban areas. The understanding of three-dimensional behaviour of pollutants around buildings will permit, among others, to limit the ingestion of polluted air into the heating, ventilation and air conditioning system (HVAC) that can produce a significant degradation of air quality in the work place.

The main conclusions of the present study can be summarized as follows:

- In general, the results confirm that the pollutant plume behaviour can be successfully detected using steady CFD approach. However, an underestimation of pollutant dispersion especially in regions with high turbulence activity has been observed. This is likely due to the RANS incapacity of detecting flow unsteadiness.
- Comparisons between wind tunnel data and CFD simulations based on steady RANS (using Realizable turbulence model) confirmed that results follow a satisfactory trend (qualitative agreement) even though CFD underestimates dilution in the vicinity of the source.
- Pollutant dispersion from a rooftop stack is greatly influenced by the value of turbulent Schmidt number (Sct). It was confirmed that low values of Sct may partly compensate for the underestimation of dispersion, by increasing species diffusion. A better agreement in terms of trend with wind tunnel data is generally observed at Sct = 0.3 for all cases. The choice of a suitable Sct requires a careful assessment of vortical structures in the built environment.
- The scaled residual value analysis revealed that the criterion to stop a calculation is very important, particularly for a non-isolated building configuration. The current study established that all equations should reach a residual value of 0.4×10^{-5} to minimize the influence of this parameter in the final solution.
- CFD provides valuable information about scalars and velocity fields as well as about vortical structures formed in the leeward side and between buildings. Knowing how these flow characteristics interact with the surroundings is essential to improve the understanding of pollutant dispersion within an urban area.
- Unsteady RANS (URANS) methodology did not show any substantive improvement of the CFD estimates when compared to the RANS approach, as opposed to the LES approach, which does improve the CFD predictions, albeit at a high computational cost.

5.1 Recommendations for future research

The present study focused on steady RANS approach for isolated and non-isolated building configurations. However, a systematic underestimation of dispersion produced by RANS was found. This underestimation is likely due to the inherent incapability of RANS to detect unsteadiness of airflow around buildings. A comparison with LES approach revealed, as expected, a better agreement with wind tunnel data; but at a very high computational cost. This makes the LES approach much less affordable, particularly for parametric studies. For future research, it is therefore suggested to evaluate a hybrid RANS/LES technique, which is a transient model combining the beneficial approximations of the RANS approach, applied close to the walls, with the LES technique for the rest of the domain.

The results presented in this report included a few non-isolated configurations to evaluate the applicability of CFD in urban dispersion studies. The natural follow-up step would be to extend the present research to include more complex configurations with realistic geometries in order to improve the understanding of pollutant aerodynamics in urban areas.

REFERENCES

ASHRAE 2011. Chapter 45, Building Air Intake and Exhaust Design. ASHRAE Applications Handbook, American Society of Heating, Refrig. And Air-Cond. Eng., Inc., Atlanta, USA

Blocken, B., Stathopoulos, T., Saathoff, P., Wang, X., 2008. Numerical evaluation of pollutant dispersion in the built environment: comparisons between models and experiments. Journal of Wind Engineering and Industrial Aerodynamics, 96, 1817- 1831.

Brzoska M., Stock D., Lamb B., 1997. Determination of plume capture by the building wake. Journal of Wind Engineering and Industrial Aerodynamics, 67/68, 909-922.

Castro I.P., 2003. CFD for External Aerodynamics in the Built Environment. The QNET-CFD Network Newsletter, Vol. 2 No. 2.

Cermak, J.E., Davenport, A.G., Plate, E.J., Viegas D.X., 1995. Wind Climate in Cities. Kluwer Academic Publishers, NATO ASI Series E vol. 277, The Netherlands.

Chavez, M., Hajra, B., Stathopoulos, T., Bahloul, A., 2012. Assessment of near-field pollutant dispersion: Effect of upstream buildings. Journal of Wind Engineering and Industrial Aerodynamics, 104/106, 509-515.

Chavez, M., Hajra, B., Stathopoulos, T., Bahloul, A., 2011. Near-field pollutant dispersion in the built environment by CFD and wind tunnel simulations. Journal of Wind Engineering and Industrial Aerodynamics, 99 (4), 330-339.

Cheng Y., Lien F.S.,Yee E., Sinclair R., 2003. A comparison of large Eddy simulations with a standard k-ε Reynolds-averaged Navier Stokes model for the prediction of a fully developed turbulent flow over a matrix of cubes. Journal of Wind Engineering and Industrial Aerodynamics, 91, 1301-1328.

Di Sabatino, S., Buccolieri, R., Pulvirenti, B., Britter, R., 2007. Simulations of pollutant dispersion within idealized urban-type geometries using CFD and integral models. Atmospheric Environment, 41, 8316–8329.

Flowe, A.C., Kumar, A., 2000. Analysis of velocity fields and dispersive cavity parameters as a function of building width to building height ratio using a 3-D computer model for squat buildings. Journal of Wind Engineering and Industrial Aerodynamics, 86, 87-122.

Fluent User Guide, 2001, Volumes 1–4. Fluent Inc., Lebanon.

Franke, J., Hellsten, A., Schunzen, H., Carissimo, B., 2007. Best practice guideline for the CFD simulation of flows in the urban environment. Cost Action, 732 (Quality assurance and improvement of micro scale meteorological models). Distributed by University of Hamburg Meteorological Institute Centre for Marine and Atmospheric Sciences, Hamburg, Germany.

Hanna, S. R., Briggs, G.A., Hosker, R.P., 1982. Handbook on Atmospheric Diffusion. DOE/TIC-11223. U. S. Department of Energy, Oak Ridge, TN.

Hefny, M, Ooka, R., 2009. CFD analysis of pollutant dispersion around buildings: effect of cell geometry. Building and Environment; 44(8), 1699-1706.

Iaccarino, G., Ooi, A., Durbin, P.A., Behnia, M., 2003. Reynolds averaged simulation of unsteady separated flow. International Journal of Heat and Fluid Flow, 24, 147-156.

Li, W., Meroney, R.M., 1983. Gas dispersion near a cubical model building—Part I. Mean concentration measurements. Journal of Wind Engineering and Industrial Aerodynamics, 12, 15–33.

Liu, C., Ahmadi, G., 2006. Transport and deposition of particles near a building model. Building and Environment, 41, 828-836.

Meroney, R.N., 2004. Wind tunnel and numerical simulation of pollution dispersion: a hybrid approach. Working paper, Croucher Advanced Study Institute on Wind Tunnel Modeling, Hong Kong University of Science and Technology.

Meroney, R.N., Leitl, B.M., Rafailidis, S., Schatzmann, M., 1999. Wind –tunnel and numerical modeling of flow and dispersion about several building shapes. Journal of Wind Engineering and Industrial Aerodynamics, 81, 333-345.

Murakami S., 1993. Comparison of various turbulence models applied to a bluff body. Journal of Wind Engineering and Industrial Aerodynamics, 46/47, 21-36.

Murakami, S., Mochida, A., 1988. 3-D numerical simulation of airflow around a cubic model by means of the k-ε model. Journal of Wind Engineering and Industrial Aerodynamics, 31, 283-303.

Olvera, H.A., Choudhuri, A.R., Li, W.W., 2008. Effects of plume buoyancy and momentum on the near-wake flow structure and dispersion behind an idealized building. Journal of Wind Engineering and Industrial Aerodynamics, 96, 209-228.

Ramponi, R. and Blocken, B.J.E., 2012. CFD simulation of cross-ventilation for a generic isolated building : impact of computational parameters. Building and Environment, 53, 34-48.

Saathoff, P., Gupta, A., Stathopoulos, T., Lazure, L. 2009. Contamination of Fresh Air Intakes Due to Downwash from a Rooftop Structure. Air & Waste Management Association. 59, 343–353.

Schulman, LL., Scire, J.S., 1993. Building downwash screening modeling for the downwind recirculation cavity. Journal of the Air and Waste Management Association; 43, 1122–1127.

Simiu, E., Scanlan, R.H., 1996. Wind effects on structures: fundamentals and applications to design. 3rd Edition, Wiley Interscience Publication, USA.

Snyder, W.H., 1981. Guidelines for fluid modelling of atmospheric diffusion. EPA office of Air quality, planning and standards, Research triangle park, NC, EPA-600/8-81-009.

Stathopoulos, T., Lazure, L., Saathoff, P., Gupta, A., 2004. The effect of stack height, stack location, and rooftop structures on air intake contamination: A laboratory and full scale study. Research report R-392, Institut de recherche Robert-Sauvé en santé et en sécurité du travail, Montreal, Canada. Available online at http://www.irsst.qc.ca/media/documents/PubIRSST/R-392.pdf [Last visit: March 13, 2014].

Stathopoulos, T., Hajra, B., Bahloul, A., 2008. Analytical evaluation of dispersion of exhaust from rooftop stacks on buildings. Research report R-576, Institut de recherche Robert-Sauvé en santé et en sécurité du travail, Montreal, Canada. Available online at http://www.irsst.qc.ca/media/documents/PubIRSST/R-576.pdf [Last visit: March 13, 2014].

Stathopoulos, T., Hajra, B., Chavez, M., 2014. A Wind Tunnel Study of the Effect of Adjacent Buildings on Near-Field Pollutant Dispersion from Rooftop Emissions. Research report R-848, Institut de recherche Robert-Sauvé en santé et en sécurité du travail, Montreal, Canada. Available online at http://www.irsst.qc.ca/media/documents/PubIRSST/R-848.pdf. [Last visit: June 2014].

Tominaga, Y., Stathopoulos, T., 2009. Numerical simulation of dispersion around an isolated cubic building: Comparison of various types of k-ε models. Atmospheric Environment, 43, 3200-3210.

Tominaga, Y., Stathopoulos, T., 2007. Turbulent Schmidt numbers for CFD analysis with various types of flow field. Atmospheric Environment, 41, 8091-8099.

van Hooff, T., Blocken, B., 2010. On the effect of wind direction and urban surroundings on natural ventilation of a large semi-enclosed stadium. Computers & Fluids, 39, 1146-1155.

Wilson, D.J., 1979. Flow patterns over flat-roofed buildings and application to exhaust stack design. ASHRAE Transactions, 85, part 2, 284-295.

APPENDIX A: ADDITIONAL RESULTS FOR STACK PLACED IN THE FRONT EDGE OF THE EMITTING BUILDING

Additional comparisons for D_N between wind tunnel data and CFD when the stack is located near the front edge of the emitting building are presented in this appendix (Figure A.1). The wind tunnel data shown in Figures A.2, A.3 and A.4 come from the companion report (Stathopoulos *et al.* 2014) and the values plotted correspond to the average of M=1 and M=3. The CFD results correspond to M=1.7. All the cases use a stack 0.005m high (actual wind tunnel scale).

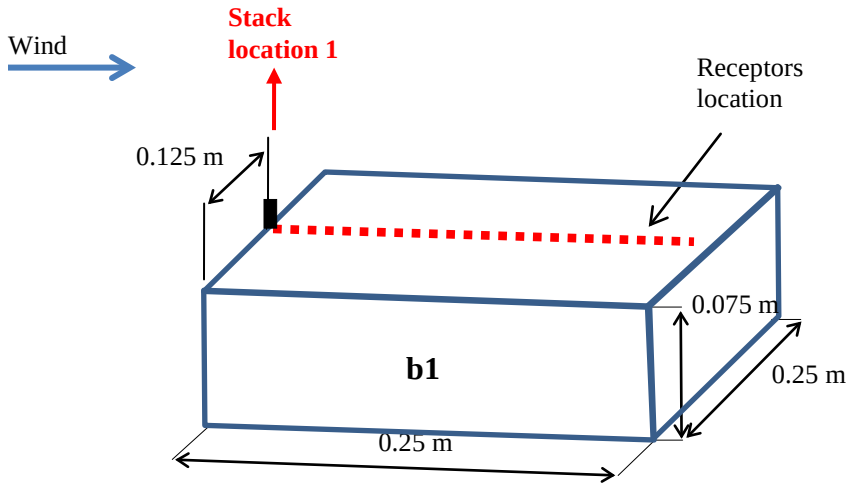

A.1 – Emitting building (b1) whit stack located in the front edge.

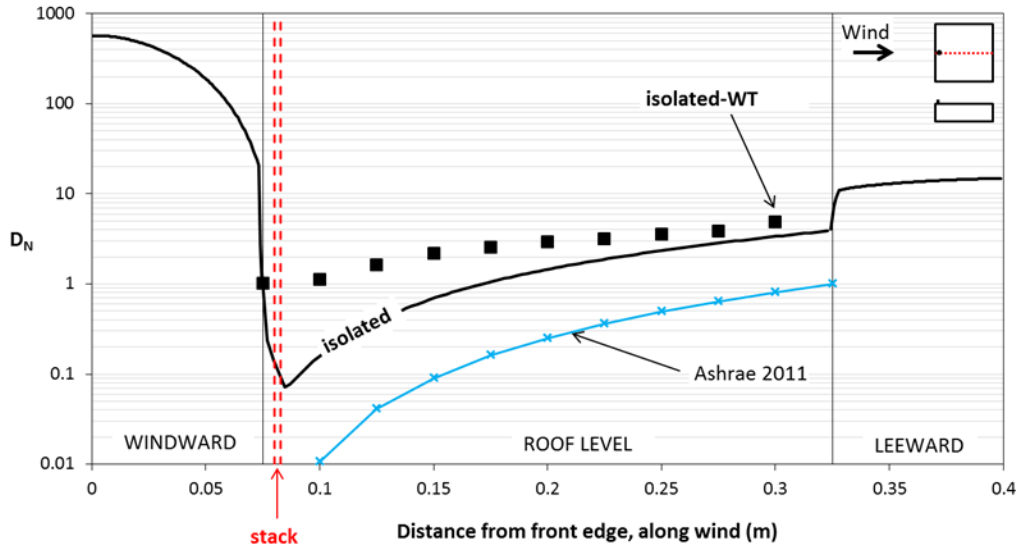

A.2 – D_N for an isolated emitting building with the stack on the edge of the roof.

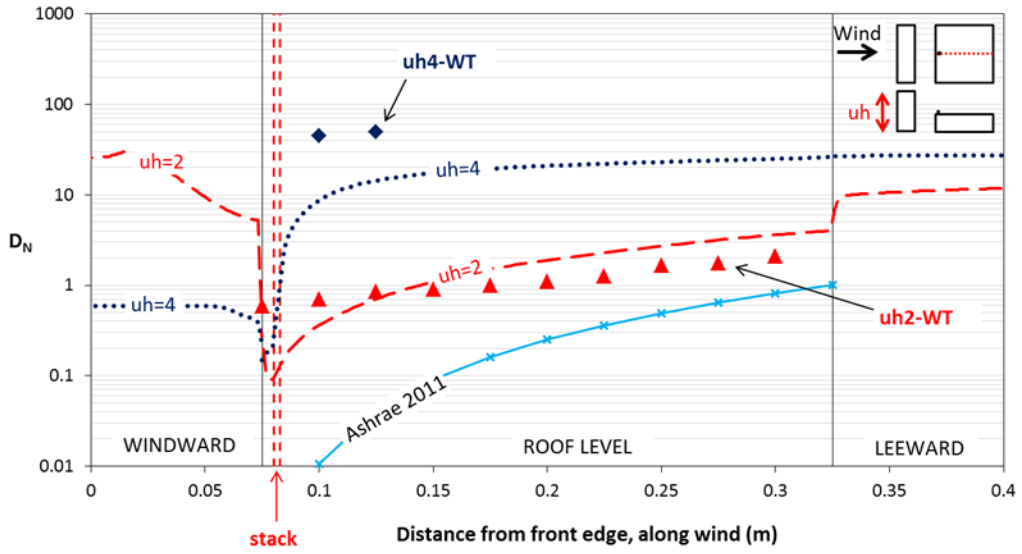

A.3 – D_N when a building is located upstream of the emitting building with the stack on the edge of the roof. Buildings uh2 and uh4 have twice and four times the height of the emitting building.

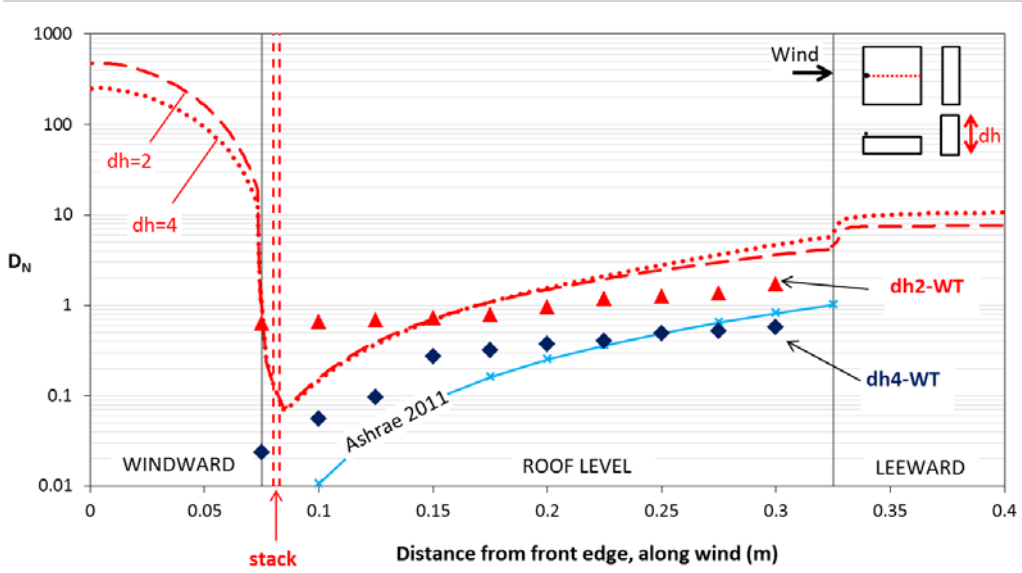

A.4 – D_N when a building is located downstream of the emitting building with the stack on the edge of the roof. Buildings dh2 and dh4 have twice and four times the height of the emitting building.

APPENDIX B: NORMALIZED DILUTION CONTOURS FOR AN ISOLATED AND FOUR NON-ISOLATED BUILDING CONFIGURATIONS

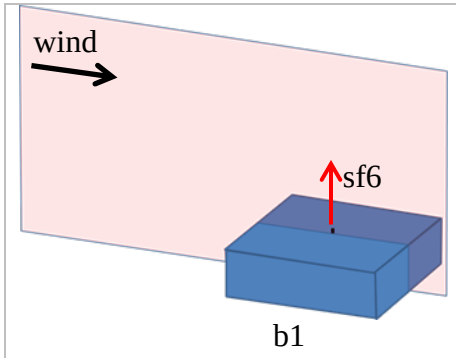

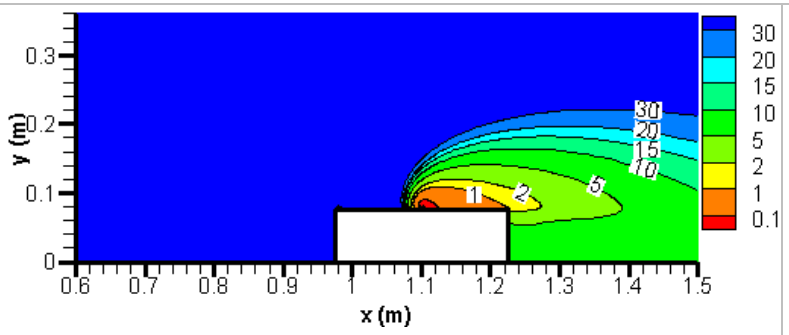

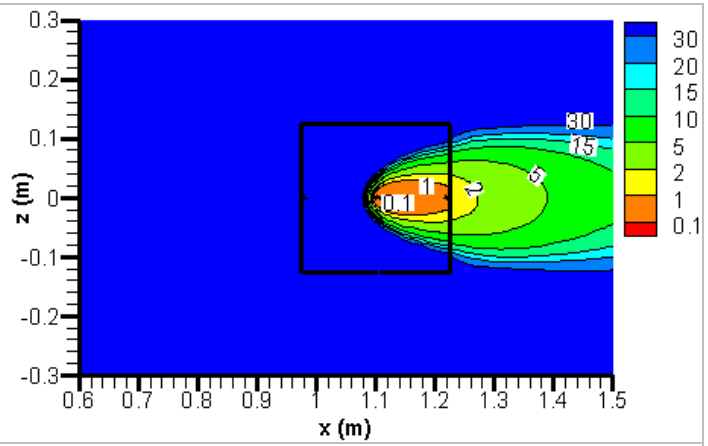

B.1(a) b1 isolated

B.1(b) Middle elevation plane, z=0 (m)

B.1(c) Horizontal plane at y=0.08(m)

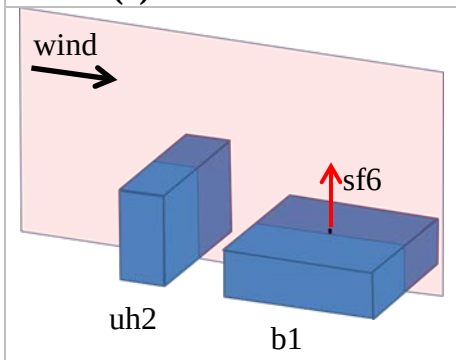

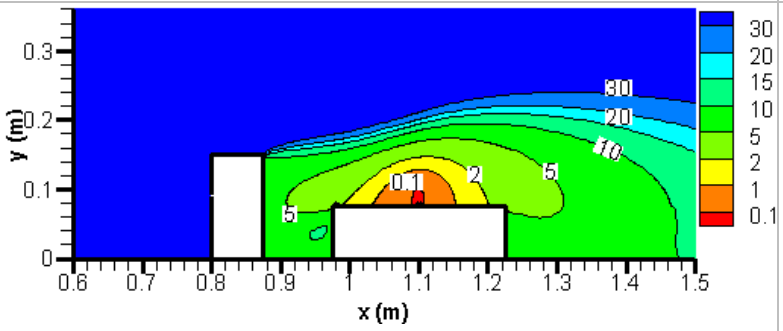

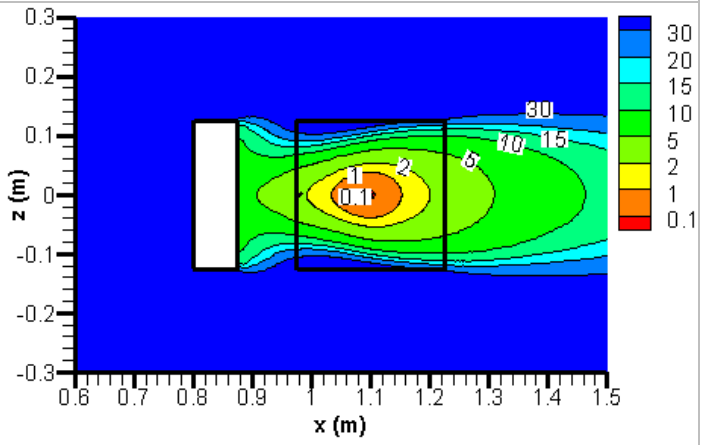

B.2(a) uh2 upstream of b1

B.2(b) Middle elevation plane, z=0 (m)

B.2(c) Horizontal plane at y=0.08(m)

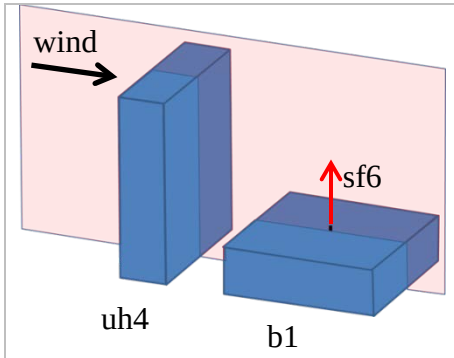

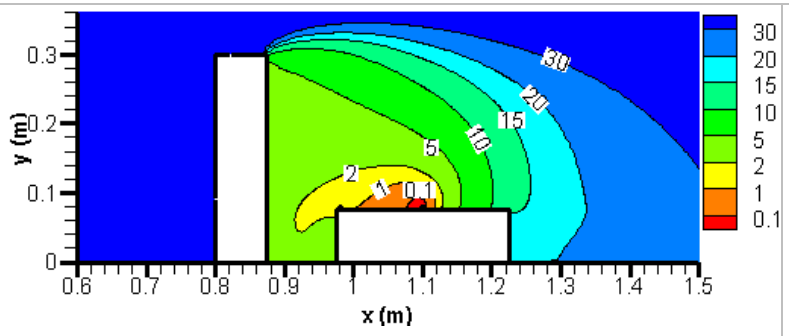

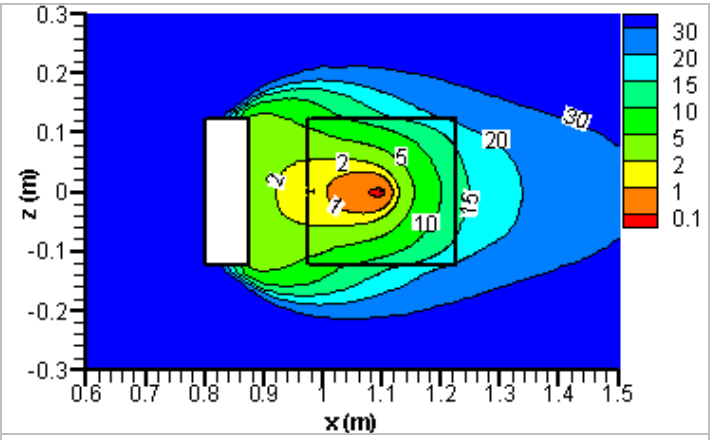

B.3(a) uh4 upstream of b1

B.3(b) Middle elevation plane, z=0 (m)

B.3(c) Horizontal plane at y=0.08(m)

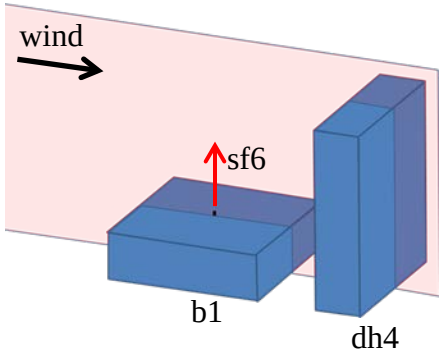

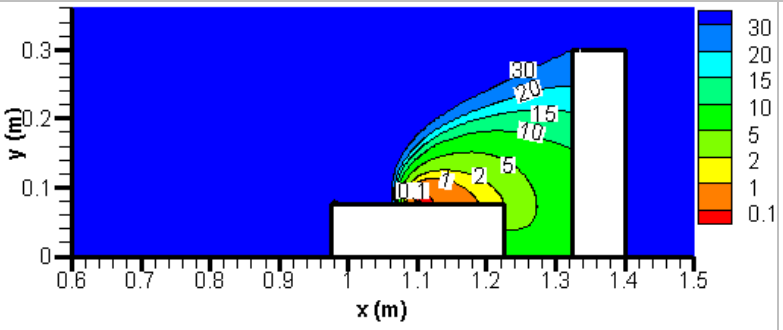

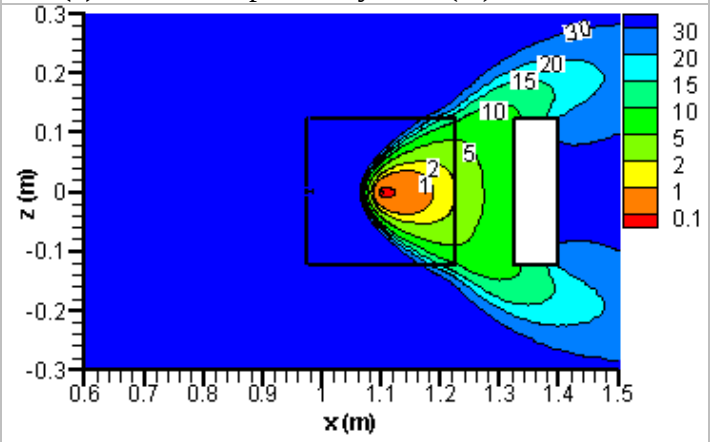

B.4(a) dh4 downstream of **b1**

B.4(b) Middle elevation plane, z=0 (m)

B.4(c) Horizontal plane at y=0.08(m)

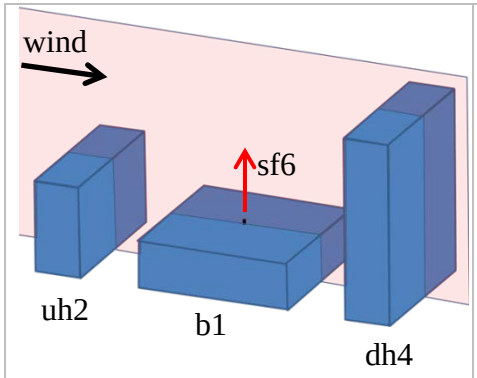

B.5(a) uh2 upstream and **dh4** downstream of **b1**

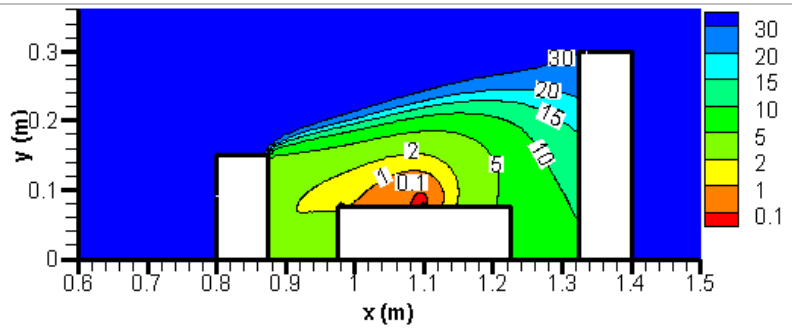

B.5(b) Middle elevation plane, z=0 (m)

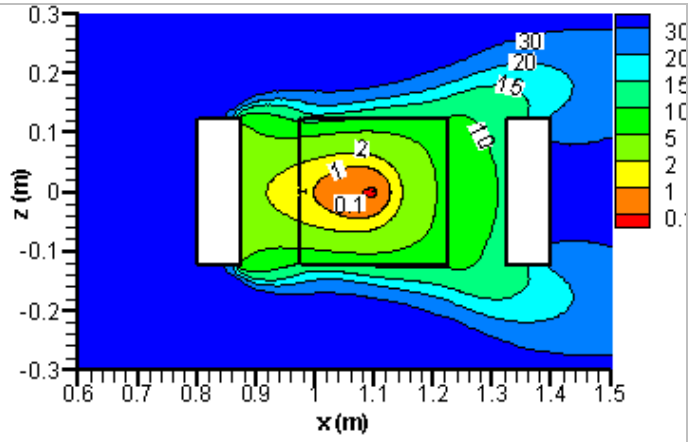

B.5(c) Horizontal plane at y=0.08(m)

APPENDIX C: STREAMLINES FOR AN ISOLATED AND FOUR NON-ISOLATED BUILDING CONFIGURATIONS

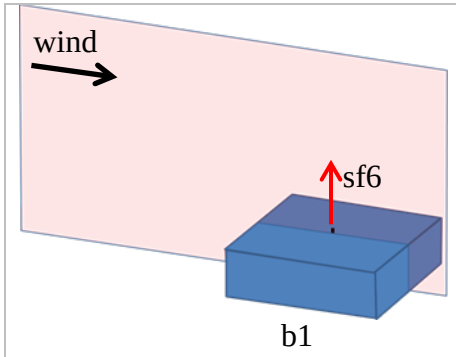

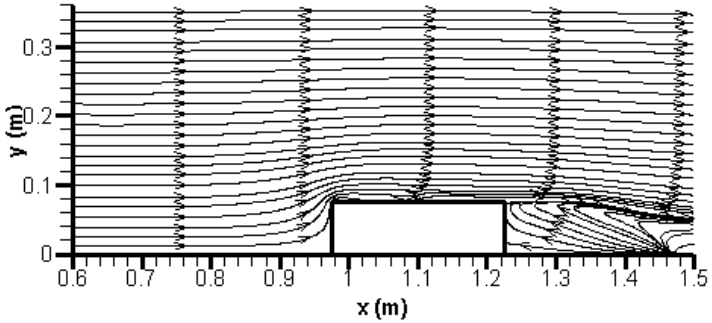

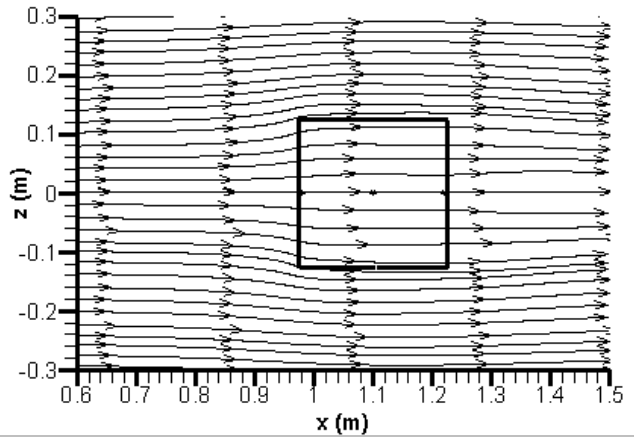

C.1(a) b1 isolated

C.1(b) Middle elevation plane, z=0 (m)

C.1(c) Horizontal plane at y=0.08(m)

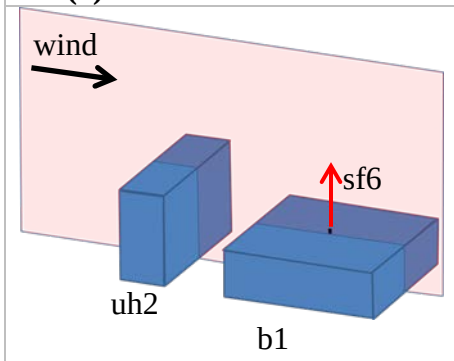

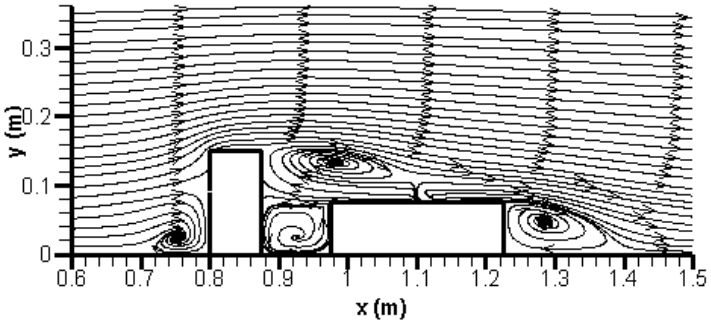

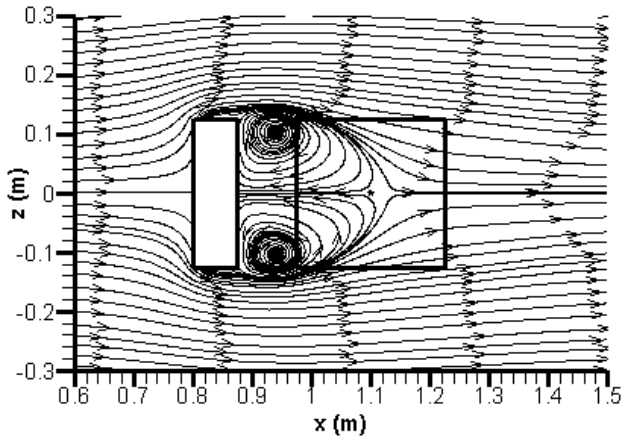

C.2(a) uh2 upstream of b1

C.2(b) Middle elevation plane, z=0 (m)

C.2(c) Horizontal plane at y=0.08(m)

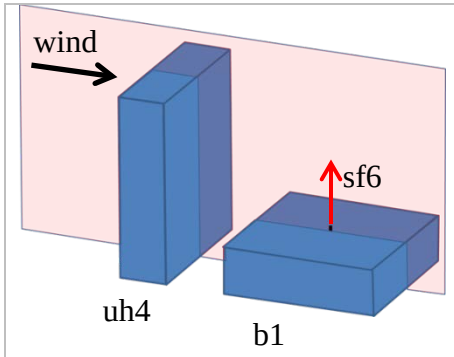

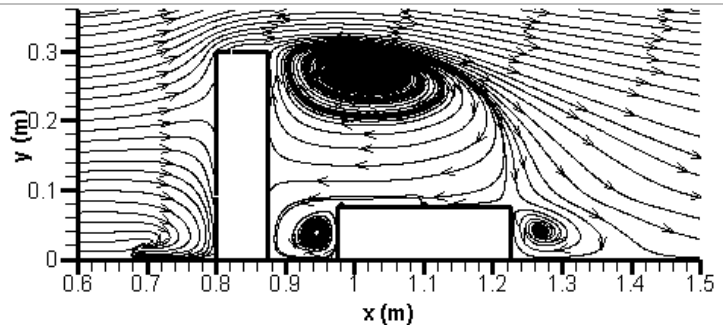

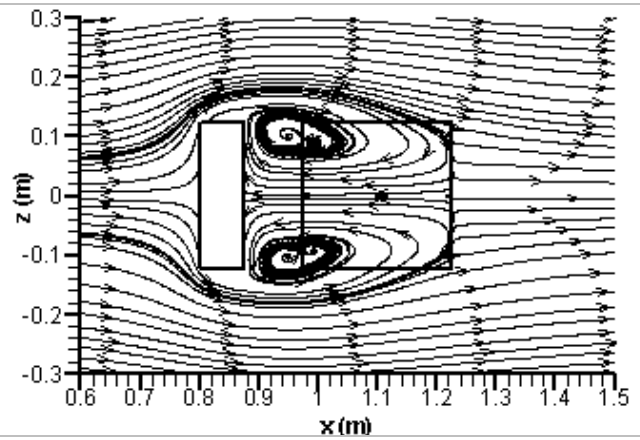

C.3(a) uh4 upstream of b1

C.3(b) Middle elevation plane, z=0 (m)

C.3(c) Horizontal plane at y=0.08(m)

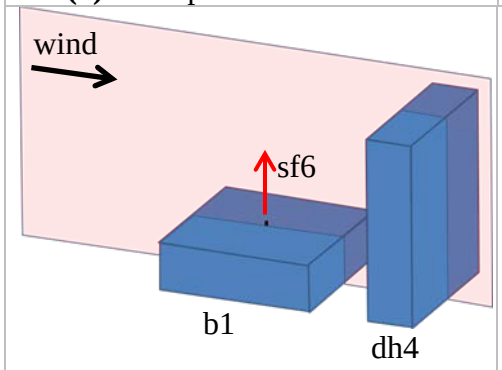

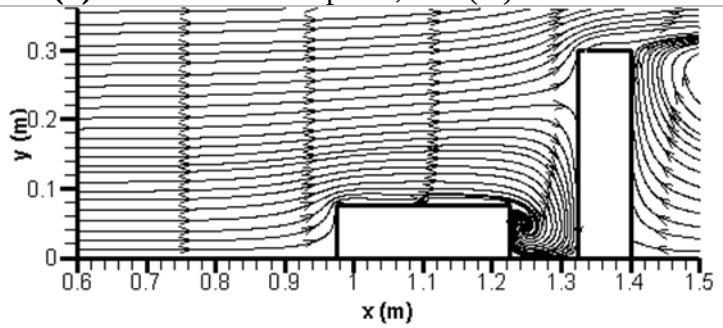

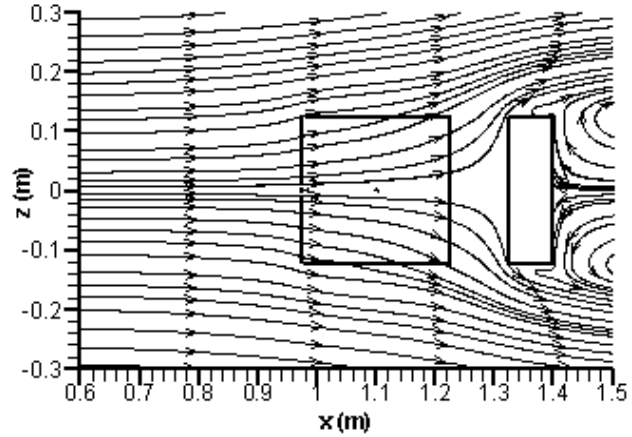

C.4(a) dh4 downstream of b1

C.4(b) Middle elevation plane, z=0 (m)

C.4(c) Horizontal plane at y=0.08(m)

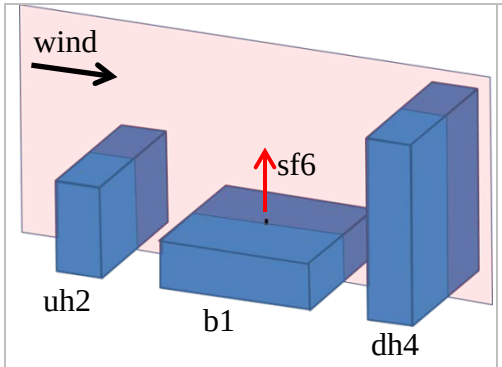

C.5(a) uh2 upstream and **dh4** downstream of **b1**

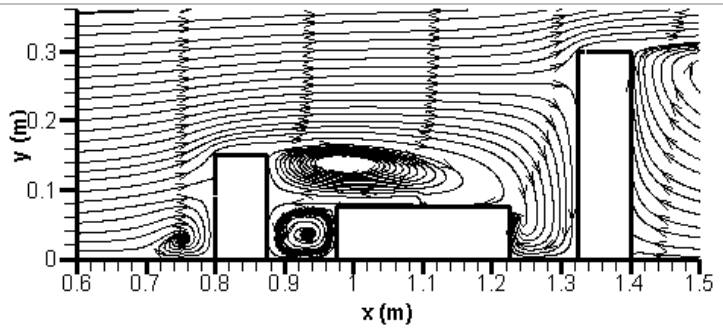

C.5(b) uh2 Middle elevation plane, z=0 (m)

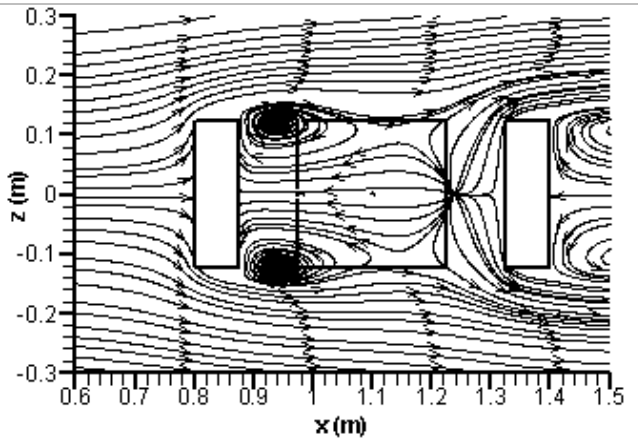

C.5(c) uh2 Horizontal plane at y=0.08(m)